FACULDADE DE ENGENHARIA DA UNIVERSIDADE DO PORTO



SAR with Active Targets

Américo José Leão da Fonseca Duarte

Mestrado Integrado em Engenharia Eletrotécnica e de Computadores

Supervisor: Sérgio Reis Cunha (PhD)

July 30, 2020

© Américo Duarte, 2020

Resumo

Radar de Abertura Sintética (SAR), é um sistema que tem como objectivo realizar observação e monitorização da superfície terrestre, obtendo imagens RADAR de alta definição, independentemente das condições meteorológicas. Tirando partido desta tecnologia, é interessante realizar o seguimento e obter informação de alguns pontos específicos de interesse na superfície terrestre. Esta dissertação propõe a projeção e construção de Tags Activas com o objetivo de serem transportadas por um portador desejado. Estas Tags Activas, que recebem, amplificam, modificam e reenviam sinais específicos recebidos por um satélite ou outro objecto voador, permitem localização e monitorização dessas mesmas Tags usando Radar de Abertura Sintética.

Este trabalho faz o estudo do uso de um sistema simples, portátil e de baixo consumo, que seja capaz the atingir grandes ganhos, de forma a facilitar a margem de *link budget* no processo que gera imagens da superfície terrestre. Para tal é proposta uma estrutura simples que transporta um *array* de seis *patch* antenas que fazem a cobertura de toda a linha de visão. Estas antenas, estão conectadas a um *power combiner/divider* que recebe, junta os sinais recebidos, e separa-os novamente para as antenas para retransmissão. As modificações introduzidas no sinal retransmitido têm dois propósitos. O primeiro é permitir uma regeneração no ganho do sinal maior do que o isolamento natural entre as antenas de receção e emissão - permitindo maior ganho sem a existência de feedback. O segundo propósito é permitir que o sistema module a informação acerca do estado de cada Tag para o sistema SAR.

A caracterização do *array* e o estudo do sistema de regeneração de sinal, bem como o seu sistema de identificação para monitorização de tags, demonstram que SAR com Tags Activas é uma tecnologia viável.

Abstract

Synthetic Aperture Radar is a system that aims to perform earth observation and monitoring obtaining high resolution RADAR images of the surface of earth in all weather conditions. Taking advantages of that technology, it is interesting to track and get information of some desired points on the earth surface. This dissertation proposes the design of Active Targets devices to be attached to specific carrier of interesting. These Active Target, which receive, amplify, modify and retransmit specific signals sent by a satellite or other airbone sensor enable locating and monitoring such targets using Synthetic Aperture Radar (SAR) approach.

This work makes a study of using a simple, portable and low power consumption system which is capable of achieving high gain in order to facilitate the link budget in the process of earth surfaces imaging. For that, a simple structure that carries an array of six patch antennas that covers all the line of sight is proposed. These are connected to a power combiner/divider that receives and couples the received signals, and decouples to the antennas again for re-transmission. The modification induced in the re transmitted has dual purposes. The first one is enable a signal regeneration gain larger than the isolation between receiving and transmitting antennas - enabling high gain without feedback oscillation. The second one is to enable the system to modulate information concerning the state of the target to the SAR system.

The characterization of the array and the study of the signal regeneration system, as also its coding system for monitoring, showed that SAR with Active Target is a feasible technology.

Agradecimentos

Ao Professor Sérgio Reis Cunha, meu orientador, por toda a disponibilidade, tempo, dedicação e compreensão, mas também por todos os ensinamentos e conhecimentos que me transmitiu ao longo de cinco anos, que me permitiram tornar numa pessoa melhor.

À Zaida pela sua presença constante, acompanhamento e suporte, e também pelo seu papel muitas vezes de conselheira, que me permitiram ultrapassar barreiras nestes anos académicos.

A todos os meus amigos que me acompanharam e me permitiram vivenciar experiências úncias, bem como todas as lições aprendidas que muitas vezes me permitiram seguir um melhor rumo. Em especial ao Carlos, David e Nuno, que me acompanharam ao longo destes anos que nunca irei esquecer, e que me permitiram traçar um caminho do qual me orgulho muito. Ao Bruno que também faz parte deste grupo, agradeço ainda toda a motivação, tempo e ajuda disponibilizada para a realização deste trabalho.

À minha família que sempre me acompanhou e apoiou incondicionalmente, e me deu todas as ferramentas e condições para que eu pudesse traçar o meu caminho com sucesso. Um especial agradecimento à Ana pela sua presença, compreensão e apoio constante.

Américo Leão Duarte

"...there is no greater joy than to have an endlessly changing horizon,
for each day to have a new and different sun"

Christopher McCandless

Contents

1 Introduction **1**
- 1.1 Context and Motivation . . . 1
- 1.2 Objectives . . . 2
- 1.3 Thesis structure . . . 3

2 Overview **5**
- 2.1 Problem and the approach . . . 5
- 2.2 SAR System . . . 7
- 2.3 Active Targets for SAR Applications . . . 10
  - 2.3.1 Feedback Issues in Active Targets . . . 13
  - 2.3.2 Patch antennas design . . . 14
- 2.4 Power Divider/Spliter . . . 16
- 2.5 Objects Identification from Orbit . . . 18

3 Target Structure **21**
  - 3.0.1 Target Layout Design . . . 21
  - 3.0.2 Target Construction . . . 22

4 Patch Antennas and Power Divider/Combiner **25**
- 4.1 Patch Antennas . . . 25
  - 4.1.1 Single Antenna . . . 25
  - 4.1.2 Antenna array . . . 29
- 4.2 Power Divider/Combiner . . . 32
  - 4.2.1 Power Divider/Combiner Design . . . 32
  - 4.2.2 Power Divider/Combiner EM Simulation . . . 35
  - 4.2.3 Power Divider/Combiner Construction . . . 37

5 Feedback Interference Cancellation and ID System **41**
- 5.1 Feedback Interference Cancellation . . . 41
  - 5.1.1 Regeneration Based on Signal Processing . . . 41
  - 5.1.2 Regeneration Based on Frequency-Shifting and Filtering . . . 42
- 5.2 ID system . . . 50

6 System Integration Results **53**
- 6.1 Target Integration and Tests . . . 53
  - 6.1.1 System Performance . . . 59
  - 6.1.2 Power Consumption . . . 64

7 Final Remarks **67**
7.1 Adversities during the work development 67
7.2 Conclusions 67
7.3 Future Work 69

A Active Target technical draw **71**

References **73**

List of Figures

2.1 Generated interference. . . . 6
2.2 SAR imaging geometry [1] . . . 8
2.3 SAR processing [1] . . . 10
2.4 SAR operation modes [1] . . . 10
2.5 Active radar calibrator [2] . . . 11
2.6 General functional transponder block diagram [3] . . . 12
2.7 Block diagram of the transponder with a digital system [4] . . . 13
2.8 Feedback oscillation of a radio repeater [5] . . . 13
2.9 Microstrip patch antenna and line feed [6] . . . 15
2.10 Recessed microstrip-line feed.[6] . . . 15
2.11 Proximity coupled feed.[6] . . . 16
2.12 An equal-split Wilkinson power divider in microstrip line form and its equivalent transmission line circuit.[7] . . . 17
2.13 ARGOS system overview [8] . . . 19

3.1 Capsule exemplar. . . . 21
3.2 Active target design. . . . 22
3.3 Active Target Molds for construction. . . . 23
3.4 Active target structure. . . . 23
3.5 Active target. . . . 24

4.1 Patch antenna design. . . . 26
4.2 S_{11} parameter. . . . 27
4.3 Antenna gain 3D plot. . . . 27
4.4 Antenna matching. . . . 28
4.5 Patch Antenna. . . . 29
4.6 Real S_{11} parameter. . . . 29
4.7 Antenna array. . . . 30
4.8 Antenna array S_{11}. . . . 30
4.9 Antenna array S_{12}. . . . 31
4.10 Gain of the array. . . . 31
4.11 Top view of the bottom layer. . . . 34
4.12 Top view of the top layer. . . . 34
4.13 Top view of the combined two layers. . . . 35
4.14 Layer distribution on the PCB. . . . 36
4.15 S_{11} parameter from simulation. . . . 36
4.16 S_{22} parameter from simulation. . . . 37
4.17 S_{21} parameter from simulation. . . . 38

4.18 Phase plot for Port1 (left) and Port2 (right). 38
4.19 Power Divider/Combiner PCB. 39

5.1 Feedback cancellation system 41
5.2 Errors form frequency shift: Symmetric Images of Target and Azimuth Error . . 44
5.3 Frequency shift and filtering block chain 45
5.4 Signal 1 at left and signal 2 at right 45
5.5 System block chain, and signals possible paths 45
5.6 Feedback path and isolation between port2 and port1 47
5.7 [1 to 1 -> isolation] and [2 to 2 -> isolation] feedback paths 47
5.8 [1 to 2 -> isolation -> 2 to 1 -> isolation] feedback path 47
5.9 [2 to 1 -> isolation -> 1 to 2 -> isolation] feedback path 48
5.10 U_{p1} band-pass filter 49
5.11 U_{p2} band-pass filter 50
5.12 Simulink block chain for simulation. 50

6.1 Antenna Array and Power Divider. 54
6.2 Active Target. 54
6.3 Measured S_{11} of Active Target 55
6.4 Measured S_{22} of Active Target 55
6.5 Measured S_{21} of Active Target 56
6.6 Schematic of the measurement of the two Vivaldi antennas 56
6.7 Schematic of the measurement of each Vivaldi antenna with the Log-Periodic Antenna 57
6.8 Schematic of the measurement between the Log-Periodic and the Active Target . 57
6.9 Graphical representation of rotation axes 58
6.10 3D Measured Radiation Pattern for Port1 58
6.11 3D Measured Radiation Pattern for Port2 59
6.12 Positioning and geometry schematic of the entire system 60

A.1 Active target technical draw. 71

List of Tables

3.1 Target dimensions 22

4.1 Antenna measurements 26
4.2 Lines Width 33
4.3 Lines Length 33

6.1 System Link Budget using 45^{o} Nadir angle 61
6.2 System Link Budget using 30^{o} Nadir angle 63
6.3 System Link Budget using 15^{o} Nadir angle 64
6.4 System Power Consumption 65

Abreviaturas e Símbolos

ADS	Advanced Design System
CNES	Centre National d'Etudes Spatiales
DSS	Digital Sub-System
EM	Electromagnectic
FPGA	Field-Programmable Gate Array
FSPL	Free Space Path-Losses
HFSS	High Frequency Structure Simulator
NASA	National Aeronautics and Space Administration
PRI	Pulse Repetition Interval
PRF	Pulse Repetition Frequency
RADAR	Radio Detection and Ranging
RCS	Radar Cross Section
SAR	Synthetic Aperture Radar
SNR	Signal to Noise Ratio
STRAPLEX	STRAtospheric Platform EXperiment
VNA	Vector Network Analyzer

Chapter 1

Introduction

Nowadays earth observation and monitoring is a very important and necessary tool for humankind that can be useful in many fields, such as meteorology, defense, oceanography, geology, and even for biology. However, and as is from the general knowledge, the space field is a recent reality. It is only necessary to go back seventy years to achieve the first efficient RADAR (Radio Detection And Ranging) for imaging purposes, that at the time, as the main emergent technology, was born for military purposes. From the need of having all-weather, 24-hour aerial remote surveillance device, the U.S. Army developed this tool that could generate images of the earth surface with any inconvenient of having the clouds in the path, or even without the daylight. A RADAR system can give images of the obstacles that reflect the electromagnetic waves, but has the concern of the limited resolution, and here, SAR (Synthetic Aperture Radar) has a great importance. The synthetic aperture that this technology creates can generate high resolution images without having a big antenna in the transmitter device.

Taking to account the advantages of earth monitoring that one can have from a SAR system, active targets can have a crucial role in terms of detecting interesting moving points that one wants to observe. It is at this point where this work intends to focus developing a low power target system that allows to follow some kind of a moving target in the earth, taking advantage of SAR technology. This can be a very interesting solution in terms of scientifically and practical purposes, such as tracking migrating animals and know firefighters location, respectively.

1.1 Context and Motivation

SAR is a technology that during the time has become a really valuable tool of earth remote sensing. It is possible to achieve high resolution images that has no dependency of weather and the flight altitude. In order to take advantages of all the capabilities that SAR has, it is possible, for example, to use it to monitoring some specific targets that one may have interest. Many fields of study has high interest of tracking specific targets that can move in earth surface. It is an example of that, the migratory paths of some animals. On the other hand, it can be also valuable in the case of tracking human positions, such as firefighters.

Targets to achieve such results may be designed to have a sufficient RCS (Radio Cross Section), in order to be possible to recognize them in the processed image. If one thinks in RCS just in terms of physical characteristics such as color, roughness, shape and size, the results may not be as good as expected. Taking that in mind, there is a need to design an active target that can receive the signal radiated from a spaceborne or airborne SAR system, regenerate and amplify the same signal, and resend it back to the spaceborn. With this process is intended to regenerate digitally the signal, in order to obtain a high gain in the emitted signal. Thinking in all this process, in the final result it will be possible to have a SAR image that may have a specific point with a greater brightness than the rest of the image, due to his high power emission, and that corresponds to the target.

1.2 Objectives

Active targets have been used in several application for recognition of a specific wanted point, or identification of an object. During this work, the main objective it will be the development of an active target unit, that can be used for SAR purposes. In this specific case, the target should be based on a system that will always be waiting to receive a RF signal that is emitted by a spaceborne or airborne SAR system, and resend it back to the SAR system with much greater gain and with an identification tag, in order to be easily detected by the system. However, there must be caution in the approach to how to have signal amplification will be carried out, and is here where resides the main challenge on this work. Many approaches can be done, for example just by amplifying the signal which could be the simplest way, but that will introduce a significant feedback which can destroy the signal that is resent back. On the other hand, a change of a frequency relatively to the received signal coudl be done, but that will generate a significant phase-shifting.

It is well known that the main difficult in this dissertation is the way to cancel the feedback introduced by the system, since the Rx and Tx signals operates in the same frequency and the Rx and Tx antennas are close to each other. With this approach, a deep study and will be done a lot of simulations and tests in order the verify the best method that can make the active target as efficient as possible. Higher gain as possible is the mandatory requirement in order to be clearly detected. Plus, once if one think in the variety of elements that may exist in the scanned area by SAR that can reflect a lot of energy, such as fences and metal roofs that have a big area, it is possible to conclude that the target has the risk of transmit less energy than this elements and be overshadowed. Also, the target unit has to be as small as possible and be portable, which induces a limited area of the Rx and Tx antennas. Low power consumption is also an important point for this target, once it is intended to make the target as efficient as possible, in order to be a competitive and interesting alternative tracking system.

1.3 Thesis structure

This thesis will be composed by seven chapters. After this chapter, that contains introductory purposes, it will be presented the problem behind this work, the approach to solve it, the state of the art, and the current state of the development of the system. In the chapter 3, it will be presented the design of the active target in terms of its structure and its construction process. The development of individual antenna and its array model to be used in the target, will be presented in chapter 4. Chapter 5 will be dedicated to the development and implementation of the digital system responsible for the feedback interference cancellation, and consequently the implementation of the ID system, that will be responsible to attribute a unique characteristic to each target, in order to be differentiated. After all the separated sub-systems are concluded, the integration analysis of the entire system will be performed in chapter 6. Chapter 7 conclude, and presents the guidelines for future work.

Chapter 2

Overview

This chapter presents an overview of the current SAR systems, some examples of active targets and its systems, mainly applied for SAR calibration, as also systems for identification systems form orbit. Also, the first approach of the overview of the problem, and a proposal to solve it will also be presented.

2.1 Problem and the approach

Nowadays there are many SAR system in operation, most of them in orbital conditions, and some others operating in certain moments flying in airplanes. Knowing the functionalities of a SAR system, that can generate high resolution images recording the back scattered signals previously emitted to the surface, it is possible to take advantage of it. One example is the tracking of specific moving points of interest using targets. This targets can be passive targets that reflects the receiving signal, not allowing a good RCS and clear identification of the moving point, taking the risk to be completely obfuscated by the surrounding environment that may reflect even more due to its big area, like metal roofs. However, active targets that amplifies the receiving signal before re-transmit it, can be used in order to improve the gain and consequently the RCS of the target. Notwithstanding, these active systems are only reliable if there is a significant isolation between the Rx antenna that receives the signal from the SAR system, and Tx antenna which re transmits the amplified signal to the SAR system, otherwise feedback oscillation can occur and will completely destroy the signal. Figure 2.1 illustrates the problem. There are many existing systems like this two, that are mainly used for radiometric calibration, as will be present later on this document.

Taking account these two systems, it is possible to understand that both are not a good solution for the purposes of this thesis, once it aims to use small and portable active targets that can have a high RCS value to be easily detected. The first one because of its low RCS that it is not enough be to detected by a SAR system, and the second one because in a small target that must be portable and placed in a human or in an animal, the isolation between the Rx and Tx is not possible.

In order to solve this problem, it is proposed in this work the development of an active target that can be small and portable enough for an animal or a human, and at the same time have high

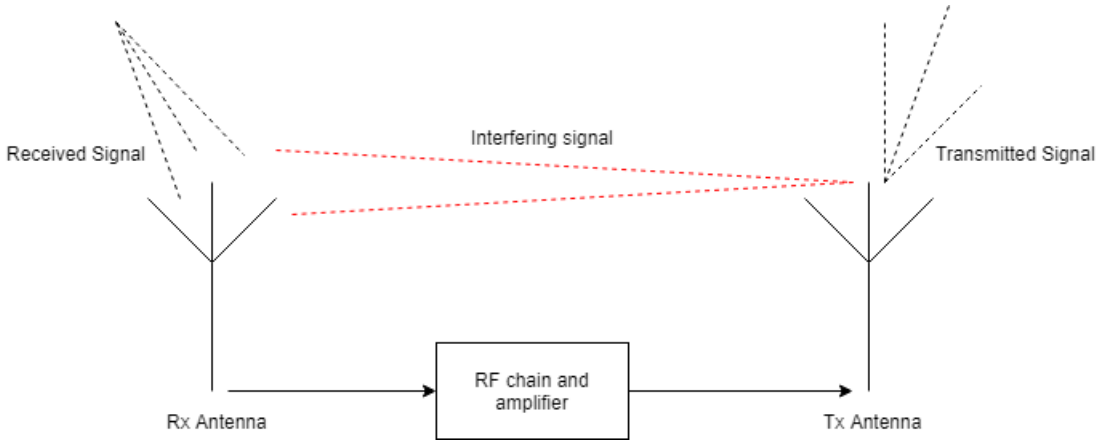


Figure 2.1: Generated interference.

RCS, in order to be detectable in the SAR image, and consequently determine its position. That it is only possible canceling the feedback oscillation generated, and constructing an array of antennas that can increase the gain and, at same time, cover all field of view. Lastly it must be implemented an identification system that allows the target to send his ID, in order to know that the point in the SAR image with greatest brightness is the active target. These three objectives must be approached in the following ways:

- In the case of the feedback problem, two different solutions may be addressed in this kind of system: The first one could be based on signal processing in which a signal should have certain characteristics in a such way that the auto correlation between them are an impulse response, and the cross correlation between the received signal and the designed signal is low as possible in order to cancel the feedback. Other option is based on frequency shift and filtering process. By doing a shift in the frequency, the feedback interference can be decrease significantly, once there is no receiving and re-transmitting at the same frequency. However, that implies a filtering system that must be capable to filter the wanted part of the signal. Consequently that will implies other processes that may be able to calculate the exactly position of the target, once the frequency shift will originate some issues in the SAR processed images, since there is a phase shift, and consequently two different positions of the target will appear.

- The antenna array will be composed by six patch antennas disposed in six sides of the active target. The active target will be a polyhedron that allows to cover the 360^{o} with great accuracy. These antennas should be designed for 2.35GHz, which is a possible SAR operation frequency, and must have a reasonable gain. Three of them will operate as Rx antennas and the others three as Tx antennas. Also a power divider for the antennas will be designed.

- Finally, it will be implemented a system that allows to the active target to send information to airborne/satellite that contains is own ID, giving information about the target that is being

detected by the SAR system and consequently in the SAR image. This information will be applied to the transmitted signal itself, which means no need to have an additional on-board computer that sends information. This can be possibly done by changing, for example, the rate at which the signal is emitted for each target, which means that each target has is own PRF (Pulse Repetition Frequency) for its emission.

2.2 SAR System

When a pulse that travels at the speed of light is transmitted, reflected by some obstacle and received again with some energy, it is possible to get information about that obstacle. A SAR system is a wide spread RADAR technique that allows to obtain high resolution images, instead of the conventional RADAR that are more limited.

This system uses a RADAR installed in a moving platform with a forward movement, that usually are airplanes or satellites, that can create a synthetic aperture, by processing the accumulated scattered signals previously emitted during the flight path. Electromagnetic pulses are emitted in a specific position of the system, and the backscattered signal will be received in a different position due to the platform movement. With this, it is possible to create a synthetic aperture that can be much bigger than the dimensions of the antenna, and allows to increase significantly the azimuth resolution that is defined as the smallest distance between two detected point targets.

A RADAR system provides an image that corresponds to a reflective map of the targets, where the bright spots are the spots with high backscattered signal, and the dark areas corresponds to the smooth surfaces. In a flight condition, the azimuth corresponds to the flight direction and the slant range to the line-of-sight. If we consider a simple RADAR system with no synthetic aperture, the azimuth resolution it is smaller and deteriorates as the range increases. In order to obtain the azimuth resolution, it can be considered the beam width as[1]:

$$\Theta_a = \frac{\lambda}{d_a} \tag{2.1}$$

where λ is the wavelength and d_a is the diameter of the antenna. Then, the azimuth resolution δ_a: [1]

$$\delta_a = \frac{\lambda}{d_a} r_0 \tag{2.2}$$

and r_0 is the range distance.

Considering an example that the range distance is 3km, the operating frequency is 2.3GHz, which means a wavelength of 0.13m, 1m antenna diameter:

$$\delta_a = \frac{0.13}{1} \cdot 3000 = 391.2 \tag{2.3}$$

which means a very low azimuth resolution, using an antenna of a considerable size.

However, in a SAR system a virtual aperture that is much longer than the physical antenna length is created due to the movement of the platform, it is possible to achieve much higher resolution. It is possible to assume that the synthetic aperture length is given by:[1]

$$L_{sa} = \Theta_a \cdot r_0 = \frac{\lambda}{d_a} r_0 \tag{2.4}$$

where

$$\Theta_a = \frac{\lambda}{2L_{sa}} \tag{2.5}$$

which leads to

$$\delta_a = \Theta_a \cdot r_0 = \frac{\lambda}{2L_{sa}} = \frac{d_a}{2} \tag{2.6}$$

In this equation, it is easy to verify that the azimuth resolution no more depends on the range, and it depends on the effective size of the antenna. Going back on the previous example, it is possible now to achieve the following result:

$$\delta_a = \frac{1}{2} = 0.5 \tag{2.7}$$

which, in this case, results in a resolution more than seven hundred times better than the regular RADAR system. Figure 2.2 represents a geometry for a SAR system.

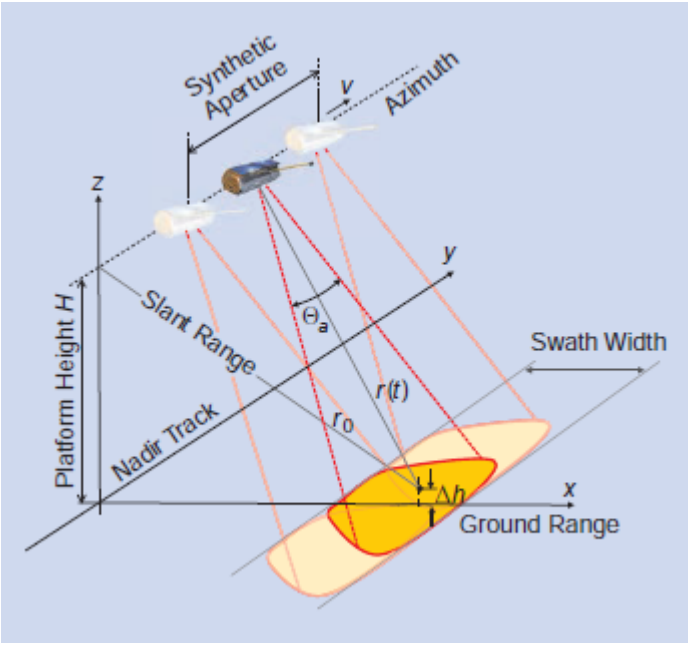


Figure 2.2: SAR imaging geometry [1]

Since the RADAR image is a two dimensional image, the second dimension is given by the range resolution, that is the same in the case of a SAR system and given by:

$$\delta_e = \frac{c_0}{2B_e} \tag{2.8}$$

where c_0 is the speed of light, and $2B_e$ bandwidth. *Chirp* signals are the signals that are transmitted by the system, and they are modulated pulsed wave forms. The pulse duration is give by τ and during that pulse duration the amplitude is constant, and the frequency is varied during the time t according to

$$f_i = k_r \cdot t \tag{2.9}$$

where k_r is the chirp rate, and the bandwidth

$$B_r = k_r \cdot \tau \tag{2.10}$$

It is also possible to define the *echo window time*, that is the time during the SAR is listening the scattered echos, and stores it. Other important concept is the PRI (Pusle Repetition Interval), that refers to the pulse repetition interval, where the pulses are transmitted and received. Its reciprocal it is called PRF.[1]

Taking into account the received signals, it is possible to say that the received echo is composed by a data matrix of complex samples. The real part corresponds to the range direction that represents also the amplitude, and the imaginary part corresponds to the azimuth, being the phase value. After receiving these signals, there is a need of processing them, once these values does not give any image information. In the processing procedure, it is first of all necessary to compress the transmitted chirp signals into short pulses. After there is a frequency domain multiplication, and each range line is multiplied in the frequency domain by the complex conjugate of the spectrum of the transmitted chirp. This process will give the information of the relative distance of the target compared to the SAR system. The second step is about the azimuth compression, where the signal is convoluted with its reference function.[1] In figure 2.3 it is possible to observe an overview of the processing of a SAR image.

There are three operations modes in SAR. The first one, and the one that will be used in the tests of this thesis is the Stripmap, the second one the ScanSAR, and the Spotlight. The ScanSAR is the mode used to obtain wider swath, where there is constantly a modification in the antenna elevation pattern, which means different angles and consequently multiples sub-swaths illuminated. The Spotlight mode corresponds to a fixed antenna pattern that illuminates for a long time a specific fixed point, which leads to a better azimuth resolution, but a small swath.[9] Finally, the Stripmap mode is the one where the antenna pattern is also fixed to one swath, but imaging a single continuous strip. This method combines the good azimuth resolution and a reasonable swath size. In 2.3 figure shows the three operation modes described above.

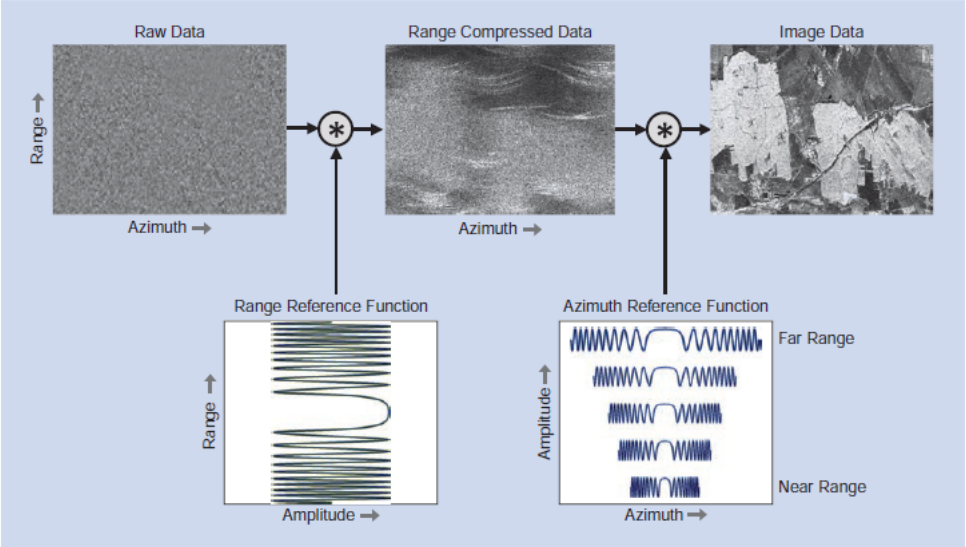


Figure 2.3: SAR processing [1]

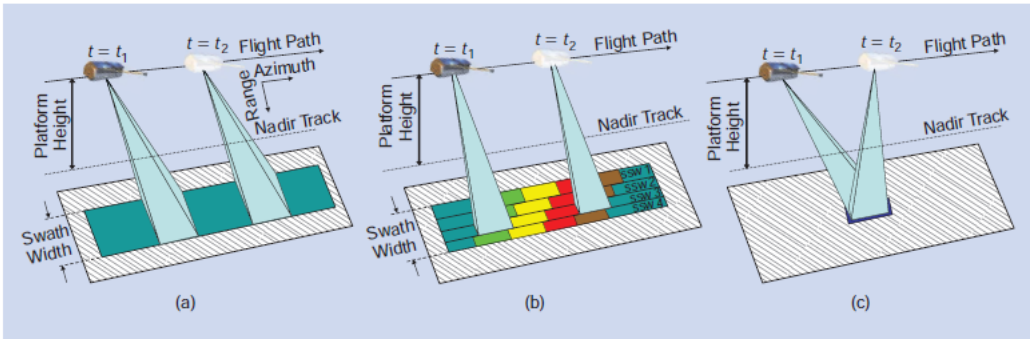


Figure 2.4: SAR operation modes [1]

2.3 Active Targets for SAR Applications

Active targets are units that are wide spread used in many kind of technologies. It is possible with that units to create many kind of responses according to the stimulation that is given. Instead of passive targets that just can reflect some signals that are received, e.g., the active target goes further, and can receive a signal and change it according its capabilities and functional purposes, and re-send it back. In the case of SAR systems, there are some point-targets that are used to calibration purposes. As these systems becomes more spread and used, there is a need to make them more accurate and capable to provide higher resolution and reliable images. Radiometric calibration is an important way to deliver image products absolutely calibrated.

There are many types of man-made reference point targets, that can be active transponders or passive corner reflectors, with known RCS.[10] In terms of radiometric calibration, the RCS is the most important feature of the target, that must be a well known value, and that also applies to the case studied in this dissertation. Since RCS is a parameter that measures how detectable an object is, it is mandatory to improve it to the maximum value as possible, in order to achieve better

detection of the unit target that is being studied. In the case of the active targets, it is possible to define RCS as:[10]

$$\sigma_a = \frac{\lambda^2}{4\pi} G_r G_a G_t \tag{2.11}$$

in which G_r is the receive antenna, G_t the transmit antenna and G_a the amplification/signal regeneration that the system applies.

Active targets calibrators for RADAR is a very used technique as an alternative to the reflectors. There are many examples of these units mainly composed by Rx and Tx antennas, as also electronics systems to amplify or regenerate the signals. Main of them are composed by an RF amplifier that increases the gain of the re-sent signal. An example of this system is shown in figure 2.5.

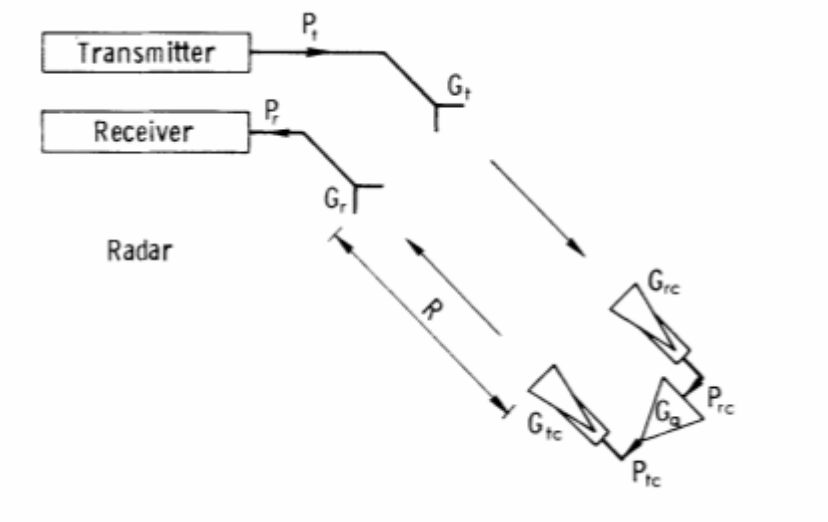


Figure 2.5: Active radar calibrator [2]

Taking into account the active radar calibrator described in the figure, it is possible to define the power received in the Rx antenna placed in the target as:

$$P_{rc} = \frac{P_t G_t G_{rc} \lambda^2}{(4\pi R)^2} \tag{2.12}$$

where

$$FSPL = (\frac{4\pi R}{\lambda})^2 \tag{2.13}$$

and R is the range distance between the target and the RADAR system, and G_{rc} the gain of the target receive antenna.

The power that is received by the active target, is amplified and re-transmitted to the RADAR, and given by:

$$P_{tc} = G_a P_{rc} \tag{2.14}$$

Finally, the power received at the RADAR system can be described as:

$$P_r = \frac{P_{tc} G_r G_{tc} \lambda^2}{(4\pi R)^2} - FSPL = \frac{P_t G_r G_t \lambda^2}{(4\pi)^3 R^4} \sigma_a - FSPL \tag{2.15}$$

In the last equation is shown why the RCS has a crucial interference in the signal received by the RADAR or SAR system. The power received is proportional to the RCS, which means, in the purposes of this thesis, a better detection of the unit.

As saw in figure 2.5, an active target can be composed by two antennas, a Rx that receives the signal sent by the SAR system, and the Tx that sends the signal back, after his amplification/regeneration, to the SAR system. Main of the calibrators for radiometric calibration in SAR systems are transponders that increases the gain of the signal received. In this cases there some advantages, such as the gain of the RF amplifiers, G_a, can be specified independently of the antenna gain, and can be smaller in order to provide wide beamwidth.[2] However, it must be considered the problem of signal interference that can be a issue, while receiving and transmitting the signal in the active target if the two antennas are too close, and there is no isolation. That will limit the gain added to the signal, otherwise, if the coupling coefficient is equal or bigger than one, the systems will oscillate and there will be feedback. As it's well known, if one increases the gain, the feedback will increase too. However this question will be discussed in other topics of this thesis.

Other active targets more complex, can be used and referenced in radiometric calibration. There are many advantages in using targets that can apply features to he signal in order to achieve higher RCS. In figure 2.6, it is possible to see a transponder that has the two Rx and Tx antennas, the receiver that down-convert the signal and send it to the DSS (Digital Sub-System) unit. This unit is capable to regenerate the signal that after will be amplified by the gain monitor, and sent to the transmitter that is an up-converted, and after re-transmitted to the SAR system. In this system, not only the gain monitor was crucial to increase the RCS, but also the DSS unit, that allowed to regenerate the signal and improve even more the RCS, making it higher and stable over the transponder lifetime.[3] The control unit it is not relevant for the purpose of this dissertation.

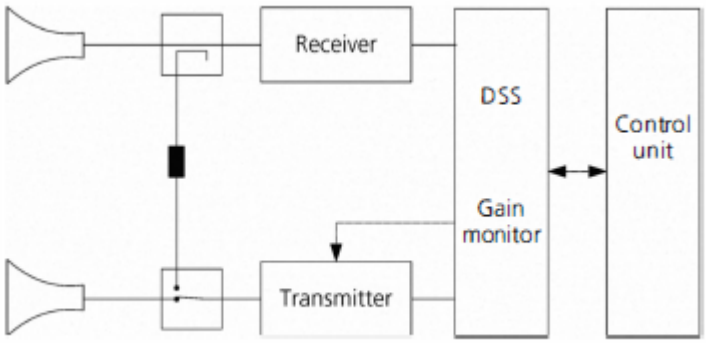


Figure 2.6: General functional transponder block diagram [3]

There are other and many examples of active targets for SAR calibration, some more complex

systems than others. As it is possible to see in figure 2.7, another system is represented where the signal is filtered, amplified and suffers a down-conversion and low-pass filter before the analog-digital conversion. There is also a FPGA (Field-Programmable Gate Array) that is responsible for the digital signal processing and storage of sampled pulses. This is the main unit where the signal suffers modification in order to perform the calibration. After this digital process there is an up-conversion and adjustment to desired RCS before passing by an high power amplifier, and re-transmitted by the antenna to the SAR system.[4]

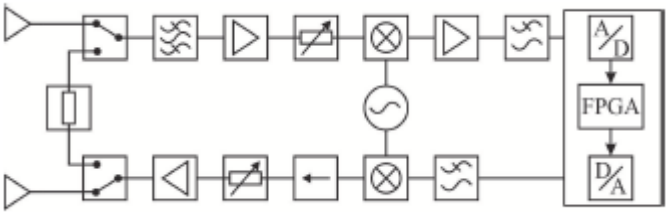


Figure 2.7: Block diagram of the transponder with a digital system [4]

2.3.1 Feedback Issues in Active Targets

When talking about transponders that receives and transmits at the same frequency, and the Rx and Tx antenna are close to each other without isolation, it is impossible to not assume that it may occur feedback oscillation. Once in this dissertation, the active targets have to be small enough to be easily transportable, it can be assumed that feedback problems will occur, because the antennas will be placed close to each other. Considering that the input signal from the SAR is amplified by the target, and transmitted back, some of the radiating signal from the Tx antenna to the SAR, it will be detected by the Rx antenna with several feedback paths with different delays.[5] Figure 2.8 illustrates a model of feedback oscillation.

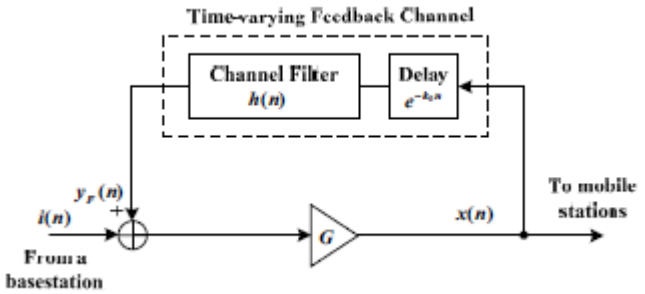


Figure 2.8: Feedback oscillation of a radio repeater [5]

The feedback can be modeled by a filter with a impulse response $h(n)$ and a delay component, k_o. The input signal is defined by $i(n)$ and the feedback signal is given by:[5]

$$y_F(n) = h(n) * x(n - k_0) \tag{2.16}$$

where

$$x(n) = G[i(n) + y_F(n)] \tag{2.17}$$

and G is the gain of the repeater.

There is a big concern in this thesis to think and implement a solution for the feedback problem that was explained above. The feedback can completely destroy the signal, and consequently become the target completely useless. In this way, the interference must be cancelled, and that is the reason for having an active target that can regenerate the signal, doing a processing where the interference is cancelled, allowing the emission of a clean signal with good RCS in order to the SAR platform be able to detect it.

2.3.2 Patch antennas design

The antennas to be used in the active targets will be microstrip patch antennas2.9. These kind of antennas are the most widely used configuration, and are very easy to analyze using transmission-line model, which is accurate for thin substrates.[11]. In terms of the design of this antenna topology, there is a need to specify information about the dielectric constant of the substrate(ε_r), the resonant frequency (f_r), and the height of the substrate h. After the specifications of these parameters, there must be calculated the effective dielectric constant, the width (W) and the length (L)[6].

The effective dielectric is essential a constant and is given by:[6]

$$\varepsilon_{reff} = \frac{\varepsilon_r + 1}{2} + \frac{\varepsilon_r - 1}{2}[1 + 12\frac{h}{W}]^{\frac{-1}{2}} \tag{2.18}$$

The width must be calculated in order to lead a good radiation efficient and is given by:

$$W = \frac{v_0}{2f_r}\sqrt{\frac{2}{\varepsilon_r + 1}} \tag{2.19}$$

in which v_0 is the free-space velocity of light.

The value of the length of the patch antenna is determined by:

$$L = \frac{1}{2f_r\sqrt{\varepsilon_{reff}}\sqrt{\mu_0\varepsilon_0}} - 2\Delta L \tag{2.20}$$

where μ_0 is the permeability of free-space, and ΔL is the normalized extension of the length which is related to the fringing effects, where electrically the patch of the microstrip antenna looks greater than its physical dimensions, and is a function of the ε_{reff}. It is given by:

$$\Delta L = 0.412h\frac{(\varepsilon_{reff} + 0.3)(\frac{W}{h} + 0.264)}{(\varepsilon_{reff} - 0.258)(\frac{W}{h} + 0.8)} \tag{2.21}$$

There are many feeding methods used in microstrip antennas. In this work, the feeding method to be used is the line feed, that consists in a feed line connected to the patch. This method is easy to

fabricate and simple to match by controlling the inset position. Figure 2.9 represents this feeding topology.

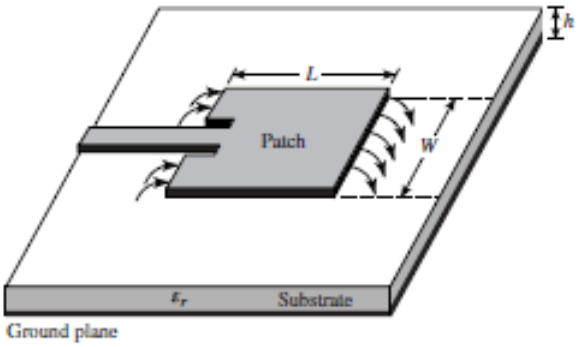


Figure 2.9: Microstrip patch antenna and line feed [6]

However, there is a need to match the patch antenna using a microstrip line feed, and that was proven that is possible to do by changing the resonant input resistance, R_{in}. This changing can be done using an inset feed, recessed a distance y_0 from the patch, as shown in figure 2.10.

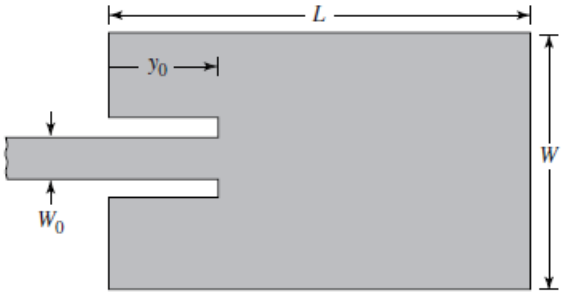


Figure 2.10: Recessed microstrip-line feed.[6]

$$R_{in} = 90\frac{(\varepsilon_r)^2}{\varepsilon_r - 1}(\frac{L}{W}) \tag{2.22}$$

The microstrip line feed is characterized by the following equations:[6]

$$\varepsilon_{eff} = \frac{\varepsilon_r + 1}{2} + [\frac{\varepsilon_r - 1}{2\sqrt{1 + 12(\frac{h}{W_0})}}] \tag{2.23}$$

and

$$Z_c = \frac{120\pi}{\sqrt{\varepsilon_{reff}[\frac{W_0}{h} + 1.393 + 0.667ln(\frac{W_0}{h} + 1.444)]}} \tag{2.24}$$

These two equations are applied only if $\frac{W_0}{h} > 1$, where W_0 is the width of the feed line, and is the case that will be adopted in this work.

Now that already all necessary parameters are defined, it is possible to calculate the value y_o that will match the patch antenna with the microstrip feed line, and is given by:[6]

$$y_0 = \frac{L}{\pi}\csc(\sqrt{\frac{R_0}{R_{in}}}) \tag{2.25}$$

As it was explained, usually the matching is performed adjusting the width of the feed line and the length of the slot. Although, it can be also performed a proximity-coupled feed, where there is a gap between the feed line and the patch antenna. Usually these techniques are implemented with two substrates where the feed line is located between them. In the case of this work the feed line must be designed as a recessed microstrip line feed, but with a space between the feed line and the patch, as it is possible to see in figure 2.11. This technique increases the bandwidth and has low spurious radiation[6].

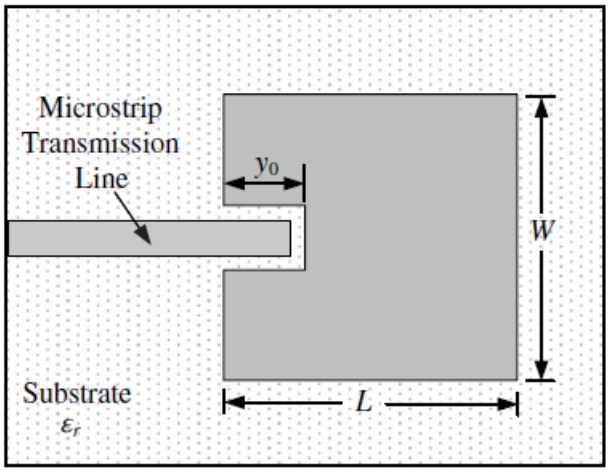


Figure 2.11: Proximity coupled feed.[6]

2.4 Power Divider/Spliter

In this work, there will be a need to use a power divider/spliter in order to combine and split the Rx and Tx signal to and from the antennas. While receiving the signal by the 3 Rx antennas, the power divider should be able to combine those, in order to be possible to process the received signal for regeneration and amplification. After that process,it will be necessary to split the processed signal to the three Tx antennas. With this concept, a 3-way Wilkinson power divider is a kind of power divider that can be use as reference in this work. This kind of passive power dividers are widely used in microwave, communications and high frequency operations, and provide simple and repeatable performance for antenna arrays. The Wilkinson power divider has completed matched output ports with good high isolation between them, and is potentially loss less. Although

it necessary to have an accurate design, once it has narrow bandwidth for cut frequency, having best performance at a center frequency[12]. This power divider, is such a solution, with the useful property of appearing lossless when the output ports are matched, that is, only reflected power from the output ports is dissipated.

The Wilkinson power divider can be designed with arbitrary power division, and with multiple output ports. Often, and as it will be done in this work, is made of microstrip line. Figure 2.12 is a illustration of a simple 1:2 Wilkinson Power Divider

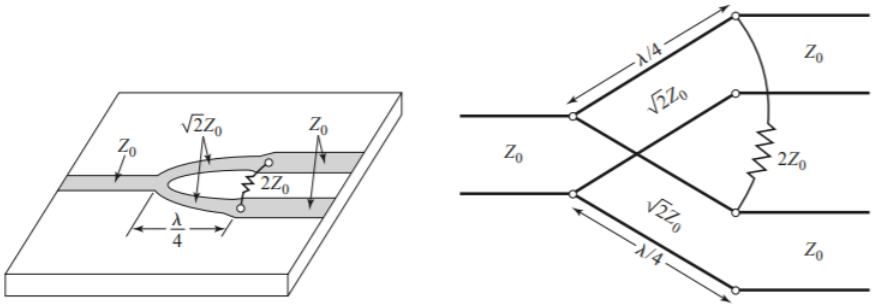


Figure 2.12: An equal-split Wilkinson power divider in microstrip line form and its equivalent transmission line circuit.[7]

When projecting the design of the power divider, there is a concern in the construction of the microstrip lines in order to have the right impedance (width) and length when thinking in the operating frequency. It is known that for an equal power spilt the lines should be designed in such a way that the load impedance (Z_L) is give by[7]:

$$Z_L = \sqrt{N} Z_O \tag{2.26}$$

where N is the number of output ports desired and Z_0 is the input impedance. Also for length calculation of the feed line, it must be considered the operating frequency that is desired for the system. In that way, the same can be achieved trough[13]:

$$L_{Z_L} = \frac{\lambda}{4\sqrt{\varepsilon}} \tag{2.27}$$

In a way to match the impedance's of all microstrip lines, a quarter wavelength approach can be used for this purpose. Also, in this kind of power dividers, a resistor is commonly used for port matching as also for ports isolation. However, and since the shape of the power divider that will be addressed in this work does not facilitates the mounting of the resistors, a quarter wavelength approach will be considered.

$$Z(\frac{\lambda}{4}) = \sqrt{Z_0 Z_L} \tag{2.28}$$

After knowing the value of the wanted impedance's is possible to obtain the size of the width of the microstrip lines, in a way that the same corresponds to the characteristic impedance's values. Equations [2.29:2.32], allows to obtain that values.

For the case: $\frac{W}{H} < 1$, where W is the width and H is the height of the dielectric:

$$\varepsilon_{eff} = \frac{\varepsilon+1}{2} + \frac{\varepsilon-1}{2}[\frac{1}{\sqrt{1+12(\frac{H}{W})}} + 0.004(1-(\frac{W}{H})^2] \tag{2.29}$$

$$Z_0 = \frac{60}{\sqrt{\varepsilon_{eff}}} ln(8\frac{H}{W} + 0.25\frac{H}{W}) \tag{2.30}$$

And considering: $\frac{W}{H} > 1$:

$$\varepsilon_{eff} = \frac{\varepsilon+1}{2} + [\frac{\varepsilon-1}{2\sqrt{1+12\frac{H}{W}}}] \tag{2.31}$$

$$Z_0 = \frac{120\pi}{\sqrt{\varepsilon_{eff}}[\frac{W}{H} + 1.393 + \frac{2}{3} ln(\frac{W}{H} + 1.444)]} \tag{2.32}$$

2.5 Objects Identification from Orbit

Nowadays, there are operating a big number of satellites, and constellation of satellites that have many purposes. Earth monitoring and observation is one of the main fields where satellites have a big impact. Many developments have been made in the last years, and tracking systems from orbit for the purposes described above is one of them. These tracking systems can provide their information and its unique ID to the satellites that are tacking them, which is important for the validation of the purposes for what they were designed. One simple example is the case of migratory animals, that with a tracking system attached to them can be followed, and consequently know more about their migratory behaviour. In this work, the active targets are also designed for that kind of purposes, which leads to a need to have a coding system that can provide the information about the active targets that are being detected by the SAR system.

There are some systems that are being used and developed at the moment, such as ARGOS system that was developed in a partnership between CNES and NASA. This kind of systems provides satellite based means to collect, locate and disseminate environmental data.[8] With this technologies the data is mainly used for applications such as meteorology, oceanography, biology, and in some cases human tracking, which are precisely some of the applications for what the active targets in this work are designed for. Systems like ARGOS are constituted by users platforms that are equipped with electronics transmitters, which corresponds in the case of this work, to the active target, by polar orbiting satellites that receives the data from the transmitters, which in the environment of this study corresponds to the RADAR. It is constituted also by a ground telemetry receiving and data acquisition stations, and by global processing centers. These last two are not directly applicable for the context of this work. It is possible to resume the function of systems like ARGOS by the following:[8]

- Incoming messages that contains information of its ID and location are sent by a user platform in sight of a satellite.

- The satellite receives the message, processes and stores it. This processing includes identification of the source, recording of the time of message reception, and measuring of the frequency of the received signal.
- These processed data is mixed with data derived from other satellite instruments, stored and sent to the ground telemetry stations when the satellite is in its sight of view. After is re-transmitted to data acquisition stations through commercial communications satellites.
- For the last, the data is decommutated and forwarded to the global processing centers where is it processed and available to the users.

Figure 2.13 represents the overview of the ARGOS system.

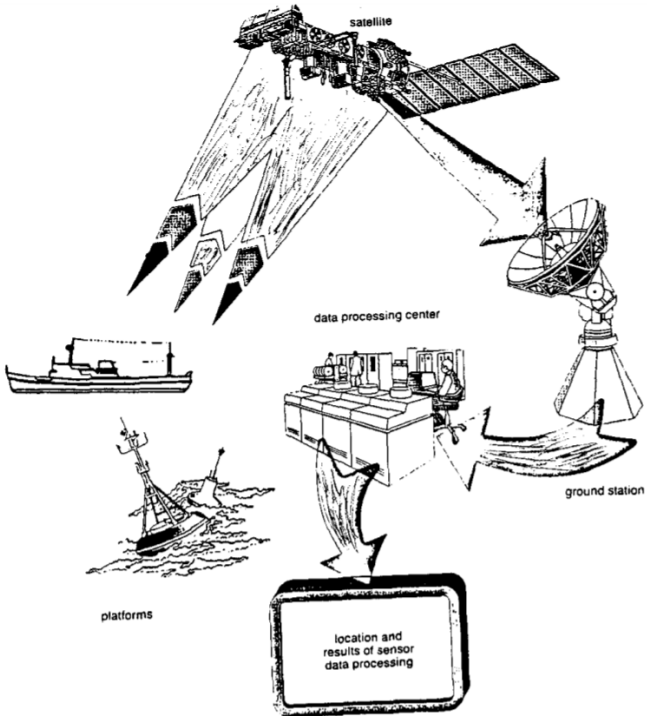


Figure 2.13: ARGOS system overview [8]

The user platforms, which are small, lightweight and low power consumption can be portable or fixed systems that vary from simple transmitters to complex system data acquisition. This emitting platform can transmits without satellite interrogation at present intervals. It has a transmission repetition period that can be set between the interval of 50 seconds do 200 seconds, depending of the complexity of the system. The messages coded in the transmission of these kind of systems may contain about some hundred of bits of information, collected by sensor data, depending if the platform may collect information of the environment and send it to the ground stations, or if it just sends its ID and location. The satellites that receives the signals from the user platform operates in a random access principle. There is a message separation in time, through synchronization, and by using different transmission repetition periods. The separation in frequency is achieved as a

result of the Doppler shift on the carrier frequency of the received signal. The acquisition of the emitter is achieved by the measuring of the Doppler shift on the carrier frequency of the received signal. [8]

There are some points in this system that makes it attractive, competitive, and useful regarding the purposes of its applications:[14]

- Low satellite altitude (800km);
- Operation service which is never interrupted;
- Antenna and transmitter needing no adjustments;
- Very little interference on the 401.65-MHz band used.
- Miniaturization: 15 to 25 grams, with batteries;
- Operate on low radiation power;
- Very low power consumption.

Nowadays there are thousands of active systems similar to this one, in which many kind of carriers are in constant motion along the earth surface, or even static. The more significant ones are drifting buoys, subsurface floats, fixed stations, terrestrial and marine animals, birds, fishing vessels and balloons.[14]

Chapter 3

Target Structure

3.0.1 Target Layout Design

Looking to my projects background in FEUP, it is possible to affirm that I have experience in stratospheric flights, namely in stratospheric balloons in the called project STRAPLEX (STRAtospheric Platform EXperiment), oriented by Dr.Professor Sérgio Reis Cunha. Many stratospheric flights have been made in the last years, using capsules of styrofoam where all the equipment is place, such as on-board computer, electronics, telemetry and experiments to validate in stratospheric conditions. These capsules have already performed many flights and still remain in good conditions, once they have a parachute incorporated, and are recovered after the flights. In order to validate the results of this dissertation, it will be performed a stratospheric flight with one of these capsules, performing passive SAR. In passive SAR, it is possible to perform a similar system to the convectional SAR, but instead of having the target in the ground, and the SAR system in flight conditions, the target is moving in a flight path, creating the synthetic aperture, and the RADAR is placed in the ground emitting the signal to the target. In that way, one of this capsules will be used to place the digital system for the signal regeneration, telemetry and batteries. Figure 3.1 is a photo of one of the available capsules, with 160mm height and hexagons side.

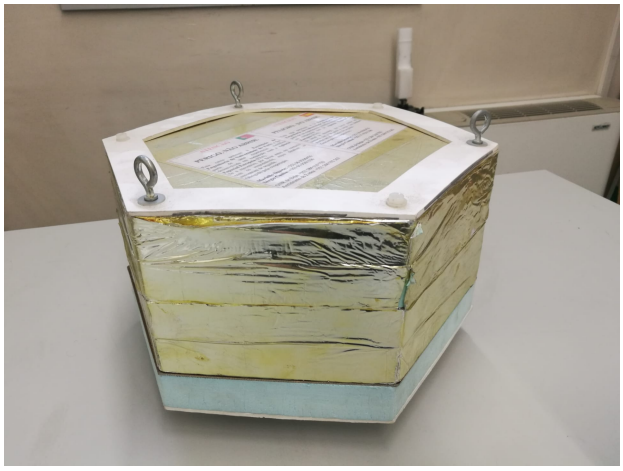


Figure 3.1: Capsule exemplar.

The active target structure that assembles the antennas and the power dividers will be constructed originally, and attached in the bottom of one of this preexisting capsules. This structure will be also made of styrofoam, once it is lightweight material and has a good performance in stratospheric conditions, as it was previously tested in many flights. This structure is a polyhedron composed of two hexagons, one in the top that is coupled to the capsule, and other one which is smaller and placed at the bottom, that is also the power divider. This allows to create six surfaces that are six trapezes with 50^{o}, where the antennas will be placed, in order to be able to receive the chirps from the RADAR placed in the ground with a good SNR (Signal to Noise Ratio). The power divider, as was told, will be also an hexagon that has two boards for signal and a shared ground. One of the boards couples the three signals from the Rx antennas, and the other board split the signal from the digital system to the three Tx antennas. The power divider will be placed on the bottom of the target, and directly soldered to the antennas, which means that one of the boards will be oriented out of the capsule. Table 3.1 have the dimensions of the active target structure.

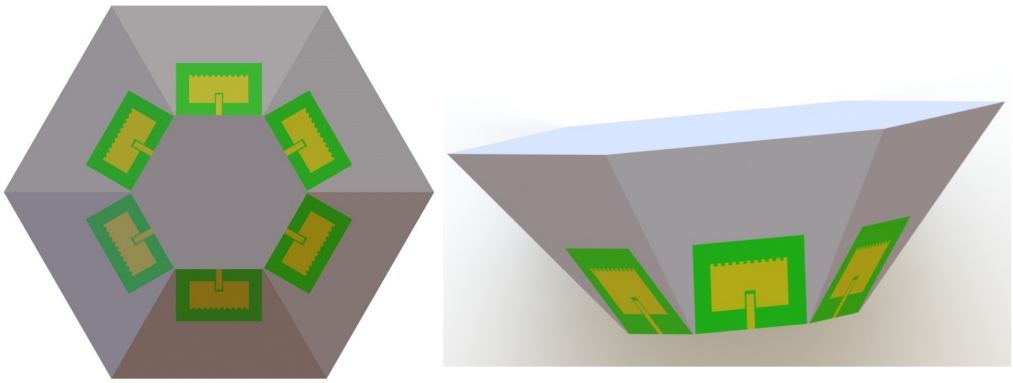


Figure 3.2: Active target design.

Table 3.1: Target dimensions

Parameter	Dimensions(mm)
Height	112.03
Top hexagon side	160
Bottom hexagon side	64
Trapeze side	146.24

In figure A.1 in the Appendix A is possible to visualize the technical draws of the active target layout.

3.0.2 Target Construction

Once the material of the target is styrofoam, the manufacturing process was done with the usage of a hot iron to cut the styrofoam with the wanted and previously made design. To be possible to use that process, there was a need to construct, first of all, molds of the target to help in the cutting

process of the styrofoam, otherwise accuracy could not be achieved. These molds were the first manufacturing step, and were made in wood at the available shops in FEUP. Figure 3.3 shows the molds that were made for target construction.

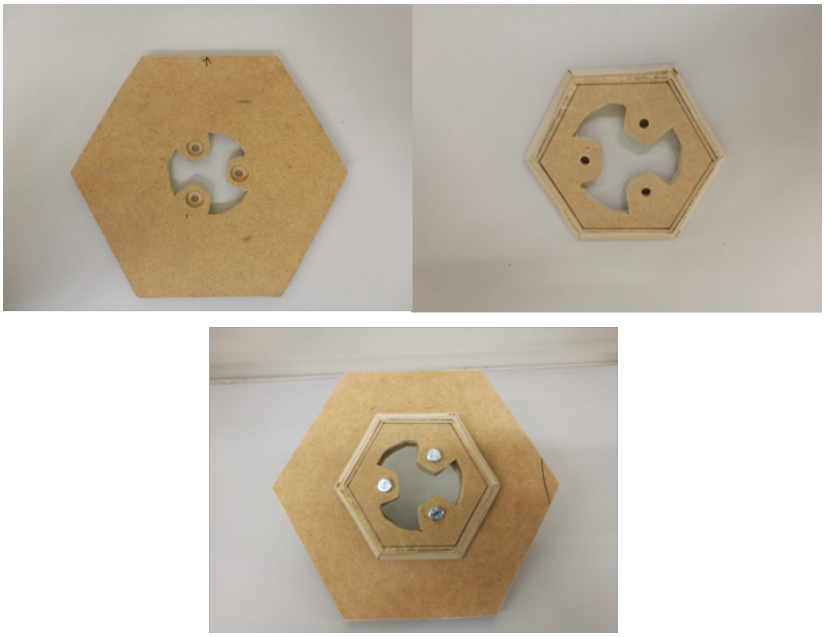


Figure 3.3: Active Target Molds for construction.

With the molds ready, the process of cutting the styrofoam could be done. The molds were attached to the styrofoam with screws, with the styrofoam placed between the two molds, and with the hot iron the styrofoam was cut with the guiding help of the molds. Figure 3.4 shows the target structure already built and ready to be assembled and mounted.

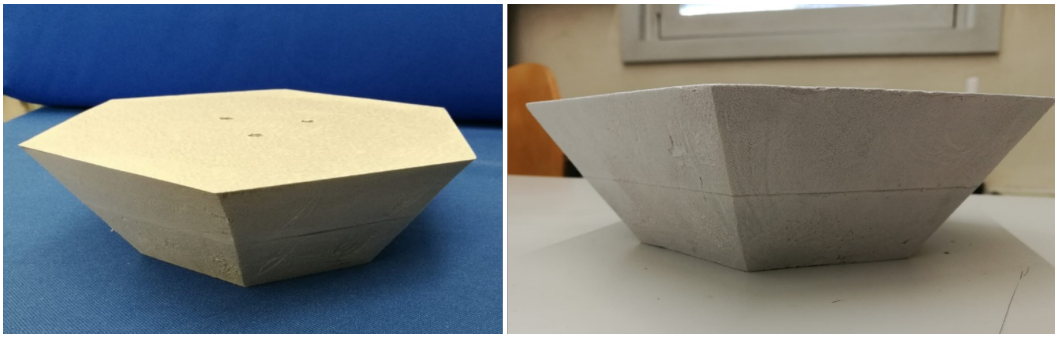


Figure 3.4: Active target structure.

After the structure completed, and also the antennas and the power divider/splitter, the unit target was assembled and mounted. The antennas and the PCB of the power divider/splitter were soldered to each other in a way to be possible to be assembled to the target structure. After, they were assembled and glued to the structure, giving a strong and robust shape to the target unit. Figure 3.5 shows different angles of the target completely assembled and ready to operate.

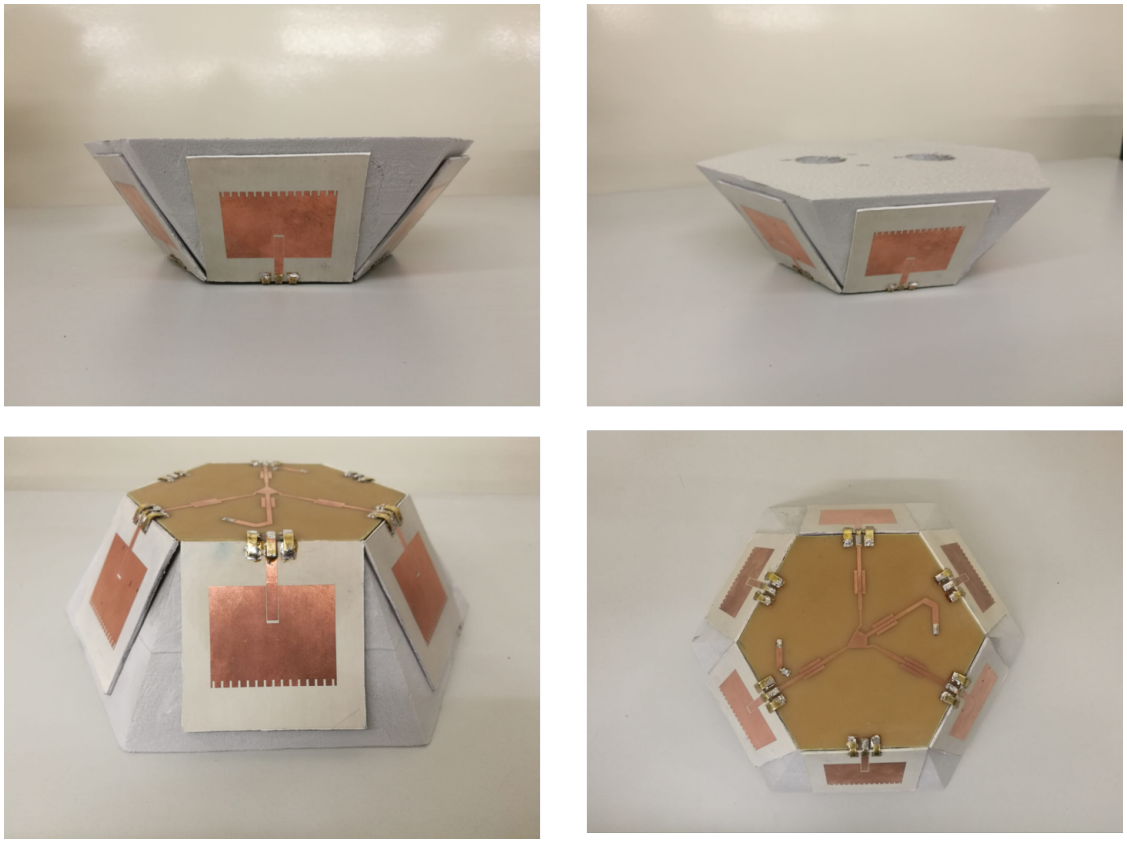


Figure 3.5: Active target.

Chapter 4

Patch Antennas and Power Divider/Combiner

4.1 Patch Antennas

4.1.1 Single Antenna

4.1.1.1 Antenna Design

The design of the antennas of the active target is based on the microstrip patch antenna design, which allows to mount it in a flat surface, and making the target more efficient in terms of portability, design, and becoming more practical for the wanted purposes. The proximity coupled feed design described on Chapter 2, it was the technique adopted for matching the feed line to the antenna, in order to take higher bandwidth and facilitate the process of matching it. The RADAR is designed for 2.35GHz, so it is necessary to design the patch antennas for this frequency. Also, as it is necessary to achieve a reasonable gain for the antennas, and the patch antennas are not the more suitable ones in terms of gain, it was chosen as dielectric the RT/duroid 6002 from Rogers Corporation, which its dielectric constant is 2.94 and height (h) 1.524mm. Firstly it was proposed to construct the antennas with FR-4 once is a cheaper material and there are many samples in the university. However, it has a higher dielectric constant, (4.4), and its high tangent losses, do not allows to obtain a reasonable gain for the antennas, being the best value obtained in the simulations only 3.5dB. Also, in order to improve the gain, it was applied to the antenna meandering edges, that provides higher gain to the antenna. This meandering edges enhance the surface area through serrations on the edge.[15] After some iteration on simulations, it was achieved the best serration layout in order to achieve higher gain.

Looking back to the equations presented in the previous chapter, it is possible to achieve the dimensions for the antenna that are shown in Table 4.1 The presented values in the table have a small difference compared to the estimated values obtained with the previous equations, once in the simulations made with HFSS, that estimated values did not presented exactly the expected results. In that way, there was a need to adjust these values in order to tune the central frequency.

In the case of the substrate dimensions, parametric simulations was successively done in order to achieve the best result, which means, a combination between the best bandwidth value and the best gain. Also the value of G which corresponds to the slot width was adjusted with parametric simulation, in order to optimize the results. Figure 4.1 represents the design of the antenna.

Table 4.1: Antenna measurements

Parameter	Dimensions(mm)
subsL	66
subsW	64
L	35.76
W	44.31
y_0	13.34
w_0	3.9
G	4.3

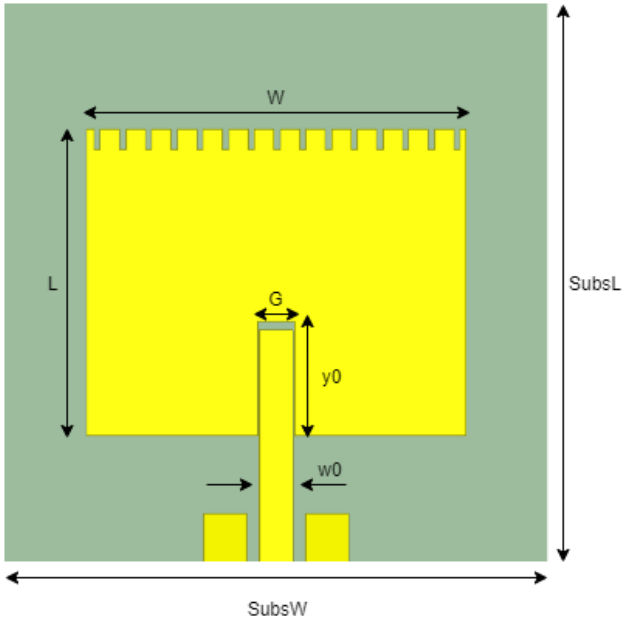


Figure 4.1: Patch antenna design.

The following figures present the simulated values for gain and bandwidth. Once at this moment is still not defined the hardware that will be used to operate as RADAR, an antenna with the higher bandwidth was designed in order to guarantee that can operate at the range of the higher bandwidth that the RADAR system can emit. That maximum value is between 50MHz-55MHz, and this antenna presents a bandwidth of 79.8MHz as it is possible to verify in the figure 4.2 that represents the S_{11} parameter of the antenna obtained in the simulation. Also, in the figure, it is possible to verify the central operation frequency for this antenna, that is 2.35GHz as it was defined in the requirements of the antenna.

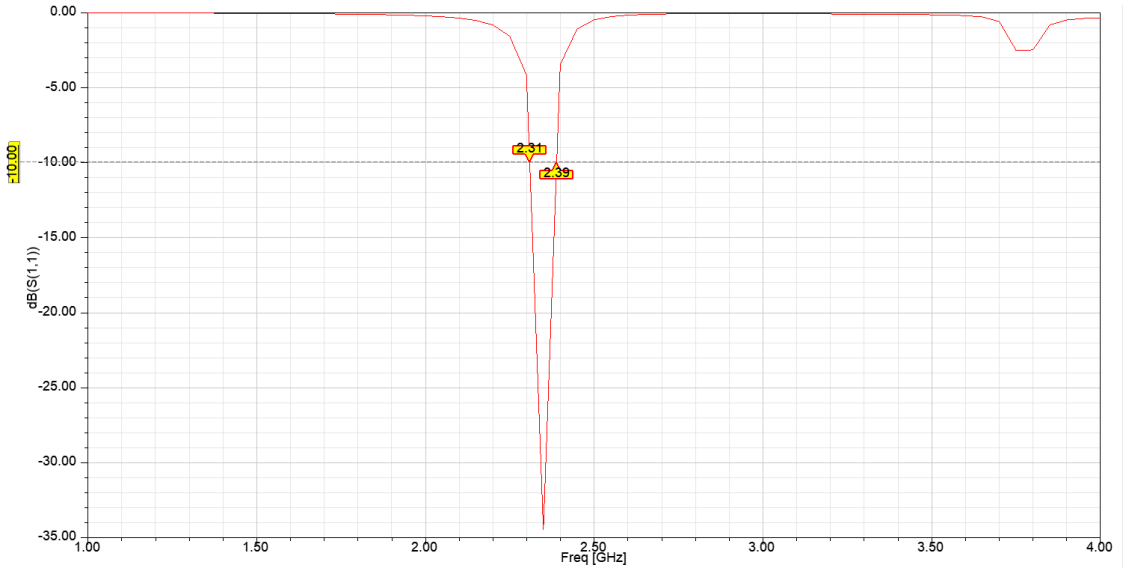


Figure 4.2: S_{11} parameter.

In the case of the gain a maximum value of $6.659dB$ was achieved, as is possible to verify in figure 4.3, which is a good value for a patch antenna, once this kind of antennas has no capability to achieve high gain. As it was explained, this gain was only possible to achieve due to the efforts of getting a better substrate for this purpose, which means, a small dielectric constant for a substrate that do not have many losses, and applying the serrations in one of the sides of the patch antennas.

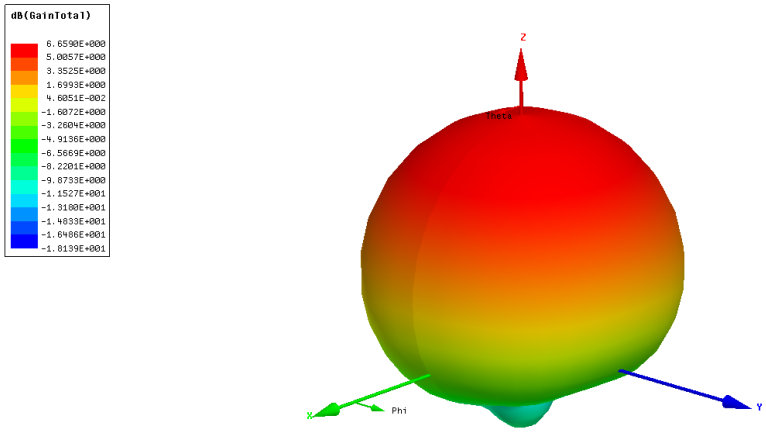


Figure 4.3: Antenna gain 3D plot.

For the last, it was necessary to ensure that the patch is matched with the feed line. First of all, analyzing the equation presented in previous chapter that gives the value of the impedance, and using the found value of w_0, the dielectric height, h, and dialectic constant ε_r, it is possible to achieve the following:

$$Z_c = 50.14\Omega \tag{4.1}$$

Analyzing now the figure 4.4, it is possible to see that the real part corresponding to the impedance of the antenna has the value of 48.16Ω, which is also close to the 50Ω. The imaginary part, as expected is almost 0. In this way it is possible to assure the matching of the antenna for the central frequency.

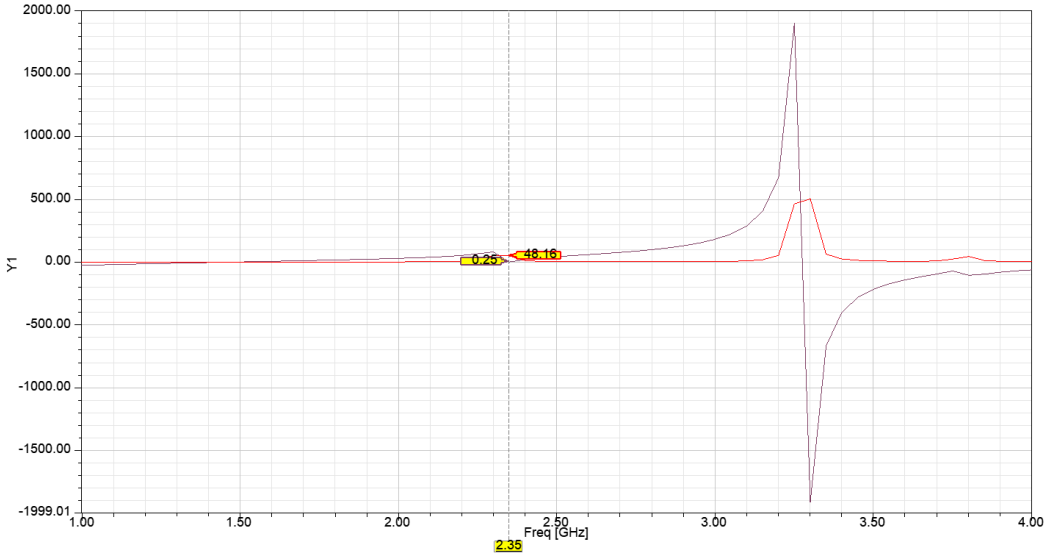


Figure 4.4: Antenna matching.

4.1.1.2 Antenna results

Once completed the simulations done in HFSS in order to the patch antenna design commit the wanted specifications , the obtained design was purposed for fabrication at the shop available in FEUP. After the cutting of the dielectric plates with the desired dimensions, the same were send to the shop forfabrication. Then, there was a need to finish the process, drilling the vias and soldering it to the ground plane. In figure 4.5 it is possible a copy of the fabricated antennas. Also, the material can have some variations on its own characteristics.

Using the VNA available at FEUP, it was possible to analyse the real S_{11} parameter of the antenna exemplar, through 4.6. The six antennas are all similar, and the behaviour of each one are really close relative to each others.

Analysing the graphic, is possible to verify that the antenna is tuned to a central frequency of 2.38GHz where S_{11} is $-16dB$. Considering the bandwidth, the same is approximately 40MHz, from 2.36GHz to 2.4GHz. Comparing these results with the ones from the simulation, it is possible to conclude that there is a shift of 3MHz in the central frequency, and the bandwidth it is smaller. This may have happen due to the fabrication process that induced some deviations from the real simulated designed.

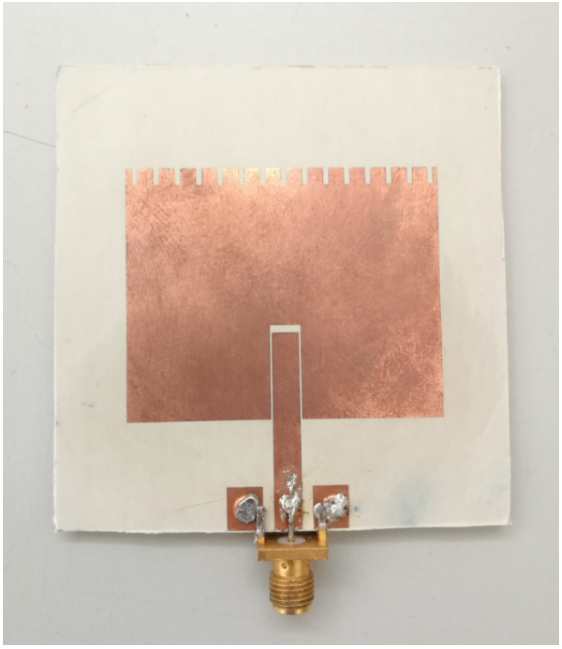


Figure 4.5: Patch Antenna.

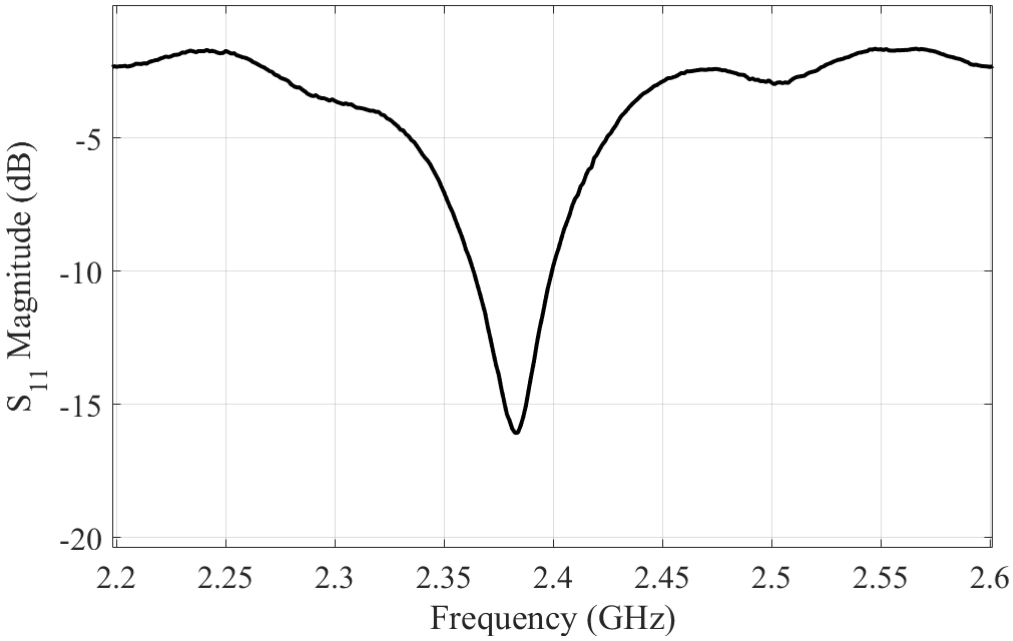


Figure 4.6: Real S_{11} parameter.

4.1.2 Antenna array

After the characterization of the patch antenna to be used in the target, it is necessary to characterize the array formed by six equal antennas. This array it forms the active target, in which three of them operate as Rx antennas and other three as Tx antennas. Using again HFSS, it was designed

an array composed by the six antennas, disposed in the wanted position with an elevation of 50º. Also, it was placed in the bottom an hexagon of FR-4 that corresponds to the power divider that will be placed in that position, in order to obtain a feasible simulation. Figure 4.7 illustrates the array exactly as it was simulated.

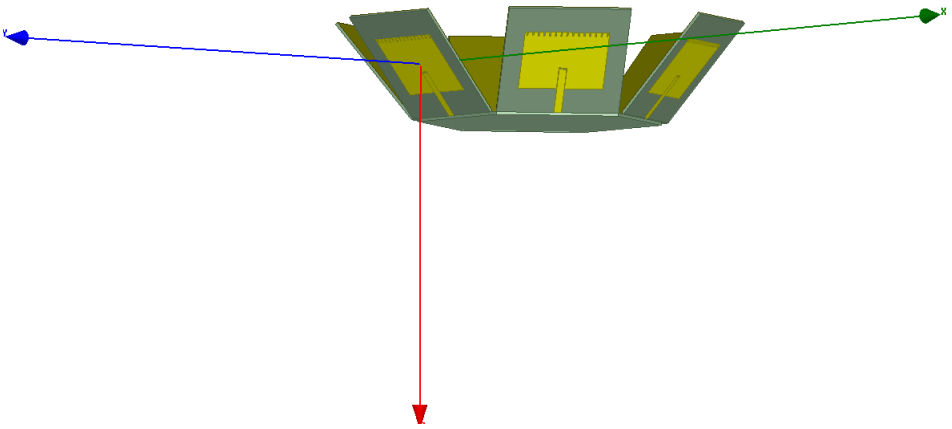


Figure 4.7: Antenna array.

The S-Parameters were also obtained for the array and each antenna had a small decrease in the bandwidth as it is expected in the case of this array of the antennas, once there is mutual coupling between elements. However this decreasing of the bandwidth is not critical since is still inside the interval, with a bandwidth of 53MHz as shown in figure 4.8. This behavior is the same for all the antennas placed in the array.

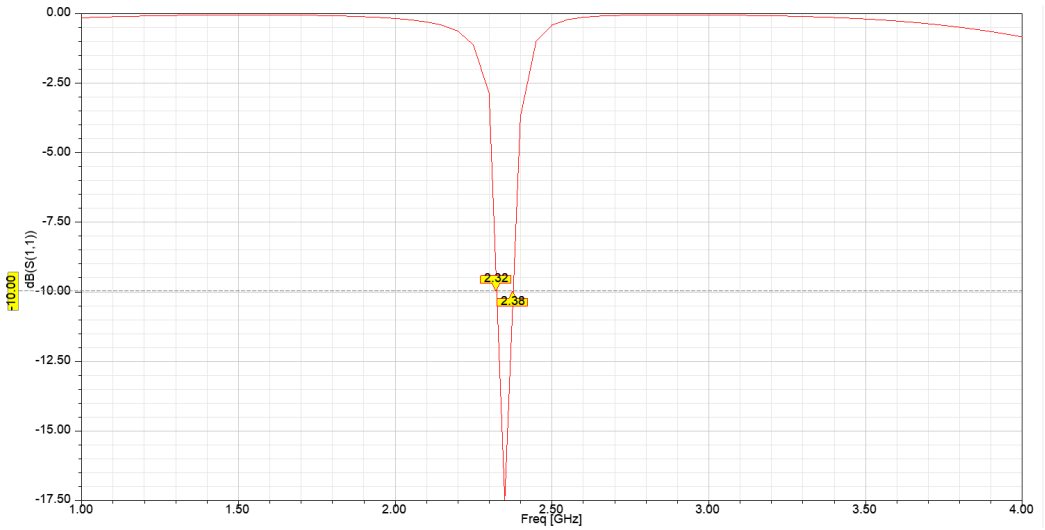


Figure 4.8: Antenna array S_{11}.

In the case of the S-Parameters that characterizes two different ports, such as S_{12}, is clearly expressed in the simulation results, that there is no cross-talk between two different antennas, once the power transferred from a port to another different one, in all of cases is less then $-20dB$, as is demonstrate in figure 4.9. This behavior was expected, because there is no common path between the antennas. These results will only be completely accurate when the power divider will be designed and integrated to the antenna array.

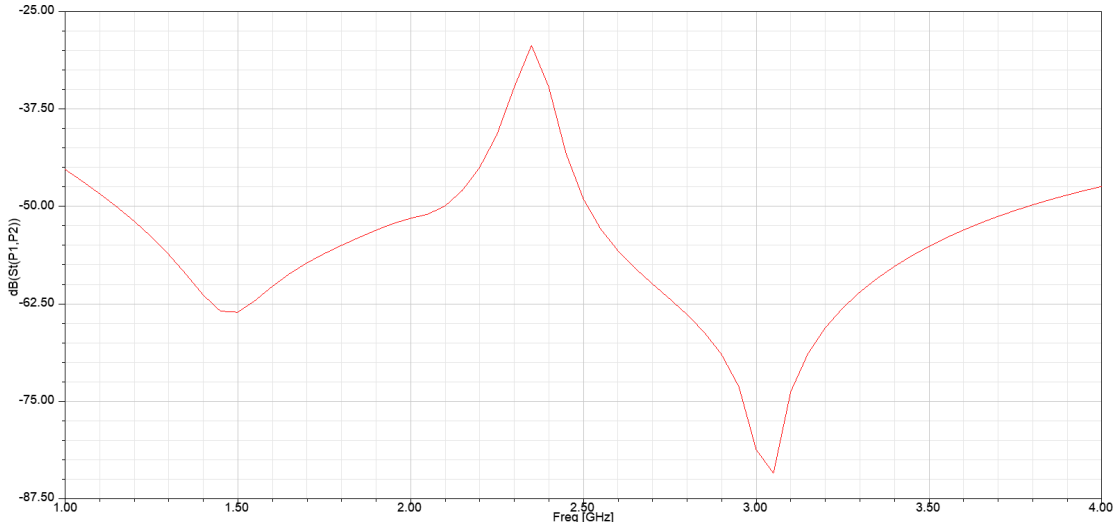


Figure 4.9: Antenna array S_{12}.

Finally the figure 4.10 presents the 3D plot of the gain of the array. Also, there is a small increase of the gain, compared to the unit antenna, achieving now the value of $6.77dB$.

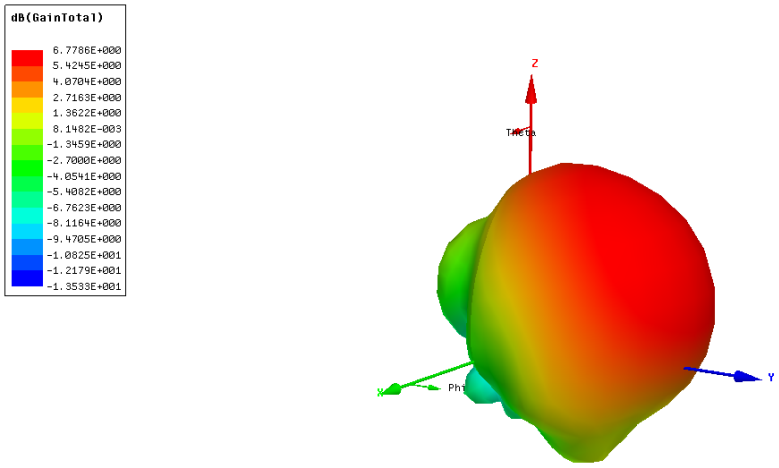


Figure 4.10: Gain of the array.

This total gain is considerable good for a patch antenna, and it will have a considerable impact in the RCS of the active target.

4.2 Power Divider/Combiner

Once the array of the antennas is composed of six antennas equal distributed in number for two different chains, one for receiving and other for transmitting it was needed to design, simulate and construct a power divider that could combine and split the RF signal. Initially it was made a design that could achieve the requirements of the system, and the S-parameters were always inserted in order to know if the result was complied with it. ADS was used to do the simulations, which is an electronic design automation software for RF, microwave and high speed digital applications.

4.2.1 Power Divider/Combiner Design

In the state of the art, it was made a bibliographic review on Wilkinson power divider, the type of power divider in each this one was based for its construction. This power divider, was designed with impedance lines in microstrip. Using the equations presented in the state of the art, it was possible to achieve the following values to the load impedance that allows to do an equal split/combine of the signal:

$$Z_L = \sqrt{3} * 50 = 86.6\Omega \tag{4.2}$$

Also, a quarter wavelength matching approach was implemented to match the impedance ($Z = 86.6\Omega$) with the line with 50Ω impedance responsible to do the connection with the antennas and the combined signal. It could be implemented in Z a matching with the terminator, designing the impedance with $\lambda/4$ wavelength. However, some adjustments in the length of the the impedance's lines in order to achieve phase accuracy were needed, and so it was made a new independent line that matches Z and the 50Ω terminator. The following equation can describe the calculation of a $\lambda/4$ wavelength:

$$Z(\frac{\lambda}{4}) = \sqrt{Z_0 Z_L} \tag{4.3}$$

Where Z_{in} is the input impedance and Z_L is the load impedance, which leads to:

$$Z = \sqrt{86.6 * 50} = 65.8\Omega \tag{4.4}$$

Considering the equations for microstrip line calculation presented in Chapter 2, it was possible to achieve the following values for each impedance:

Also, as described previously, the length of the line correspondent to the load impedance (Z_L) can be calculated by equation, 2.27 and its:

$$L_{Z_L} = \frac{0.12}{4\sqrt{4.4}} = 14.3mm \tag{4.5}$$

Table 4.2: Lines Width

Impedance(Ω)	Width(mm)
50	3.08
86.6	1.02
65.8	1.87

The remaining lengths of the lines, corresponding to the input impedance of 50Ω and to the quarter wavelength were used in such a way that could be convenient for the design in the PCB dimensions. However, and as it will be possible to verify further in this document, two of the line that are associated to the load impedance, are a little larger than the obtained valued, once it was necessary do adjustments in order to keep the phase coherence. Table 4.3 has the length values corresponding to each line

Table 4.3: Lines Length

Impedance(Ω)	Length(mm)
50	6.42
86.6	14.3
65.8	33.3

Since there was a need to have six antennas to cover the 360^{o} of the line of sight, the target bottom shape is an hexagon, which leads to the same design for the OCB

The complete PCB it is composed by two individual PCBs of FR4 with 1.6mm thickness each. At the figures below, the brown lines are placed in the bottom PCb that corresponds to the RX layer, and the yellows are placed in the top PCB, representing the TX layer.

The PCB at the bottom of the complete junction of the two PCBs carries also the ground in its top, that will be shared with the other PCB, once they will be connected. The bottom PCB is responsible to combine the signals, which leads to a design of three arms that get united at the center of the PCB, and do the coupling of the signal. There is also a fourth arm responsible to drive the combined signal to the SMA connector that will be connected to the digital system for post processing. 4.11.

The *star* design adoption was the most convenient one for the mounting of the PCB, for the distribution of the signals from and to the antennas, as also for the soldering of the SMAs connector. Many designs for the coupling/decoupling of the three lines that carries the signals were tested, including a circular junction or a simple direct connection between the three lines. These designs presented significant losses, which could be verify in the EM simulations. To attenuate that problem, a polygon that shown a good behaviour conducting the currents directly to and from the lines was designed based on the EM simulations that demonstrated less losses. However, this designed introduced incoherence's in the phase of the signals, once it is not a regular polygon and the length of the lines was not the same. In that way, there was a need to change the length of the lines in order keep the phase coherence between the signals.

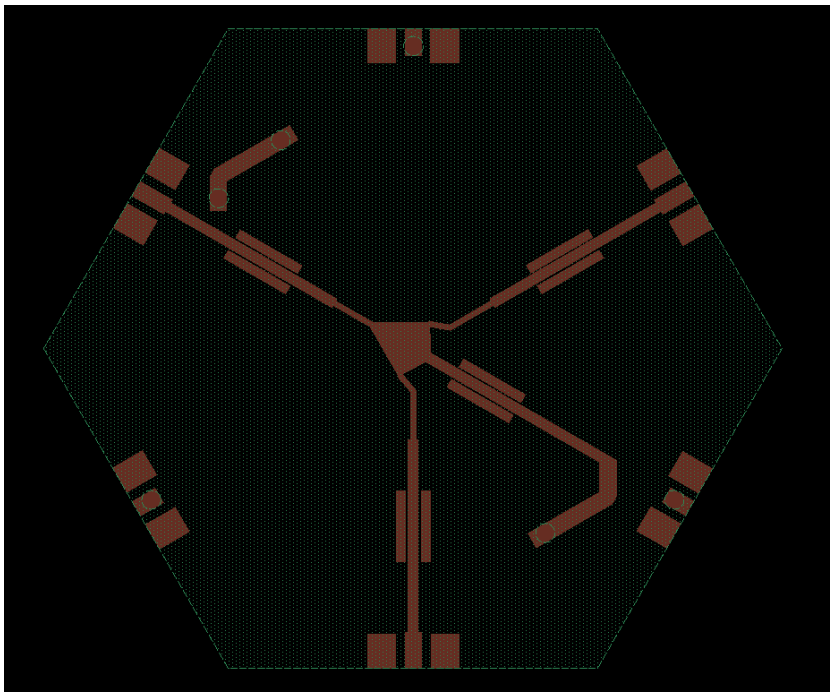


Figure 4.11: Top view of the bottom layer.

The PCB in the top, as shown in figure 4.12 have a similar design, and do the signal splitting also at the center, and split the signal to the three arms connected to the three Tx antennas.

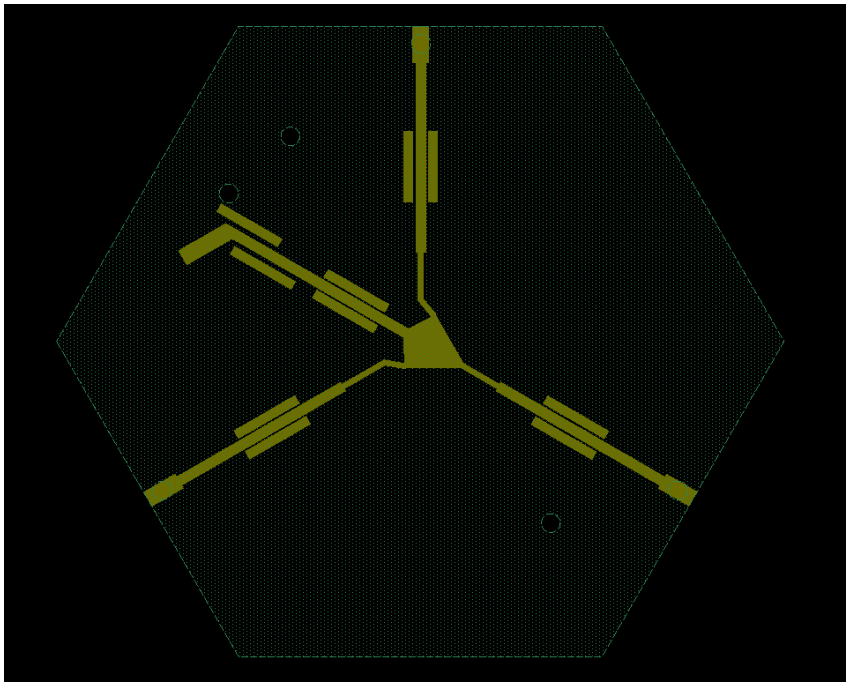


Figure 4.12: Top view of the top layer.

Figure 4.13 represents a combined "transparent view" from the top of the two layers combined and connected, creating a unique PCB when both attached. Note that this view is only possible

assuming the real connection between the layers, being the bottom layer mounted against the top layer.

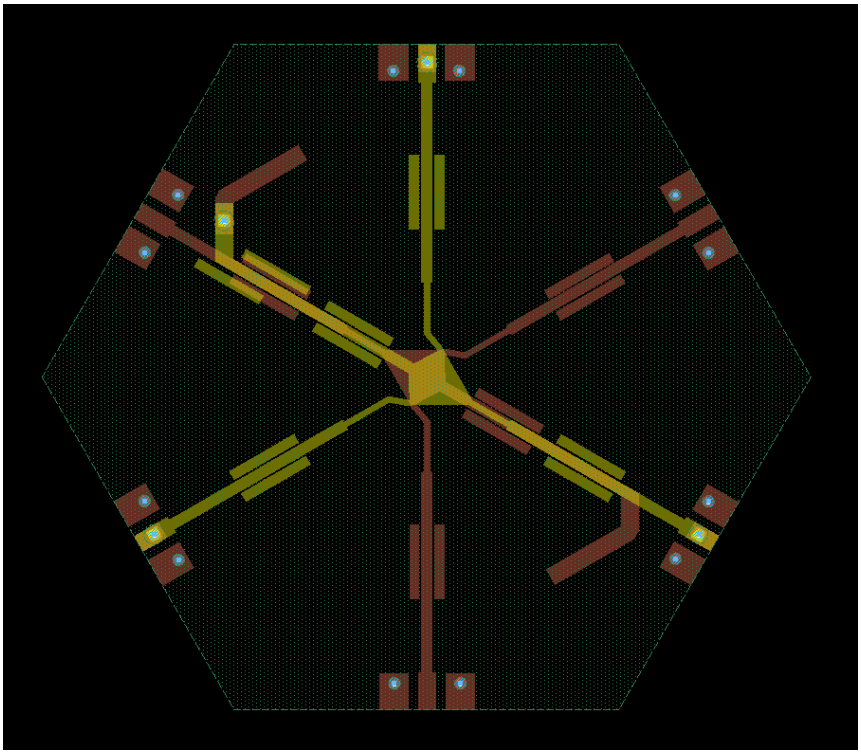


Figure 4.13: Top view of the combined two layers.

Some parasitic lines were added close to the impedance lines, in order to improve the performance of the power divider, once it allows to control the current losses on the edge of the lines.

4.2.2 Power Divider/Combiner EM Simulation

To perform a Electromagnetic simulation, the substract of the system was defined so that the two different layers could be assigned correctly. Figure represents the distribution of the layers and its connections.

The PCB is composed by two different layers of FR4 with a relative permitivity of 4.4, being each layer designed for the two independent signals. In figure 4.14, the layer *cond* is the RX layer, *cond2* is the TX layer, *pc2* is the ground that is only placed on the top layer but shared with the bottom layer, and *hole* are the vias that connects the ground layer to the lines on the top for antennas attachment, and also brings the TX signal to the top.

Many EM simulations were performed in order to verify the behaviour of the Power Divider in each relevant parameter. The main significant ones analyzed, such as S_{11}, S_{22} and S_{21}.

The S_{11}, representing the power reflected from Port1 to Port1 of the RX layer assumes the following behaviour represented in figure 4.15

It is possible to verify that the from a window of $50MHz$ of bandwidth the power is below than $-10dB$ which means that in this bandwidth it fulfils the requirements of the system. However,

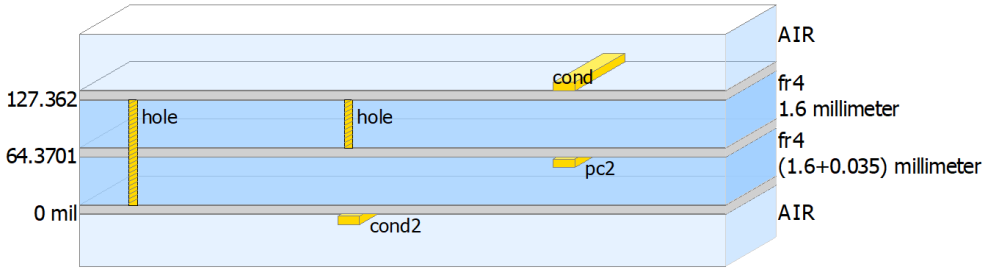


Figure 4.14: Layer distribution on the PCB.

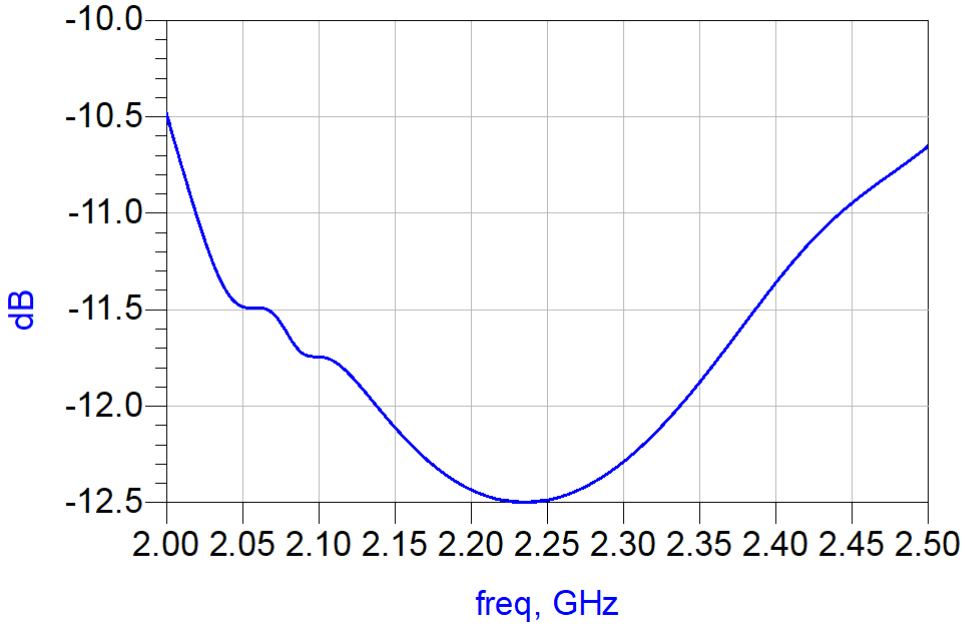


Figure 4.15: S_{11} parameter from simulation.

the operating frequency of the system, 2.35GHz it is not the frequency that has the lower power value as would be in a ideal case, being is power $-11.9dB$. Some adjustments were done in order to make the operating frequency the one with the best performance, but that adjustments made a big negative impact in other relevant parameters of the system which. Still, this would not be a concern once the frequency is inside of the window that represents a good bandwidth.

The same simulation was made for Port2 that is associated to the TX layer, where S_{22} represents the same as parameter S_{11} but for Port2. The simulation result is represented in figure 4.16

In this simulation the operating frequency, comparing to the RX layer, has a significant improvement, being the one the lower power value, and also much higher: $-32dB$. However in this

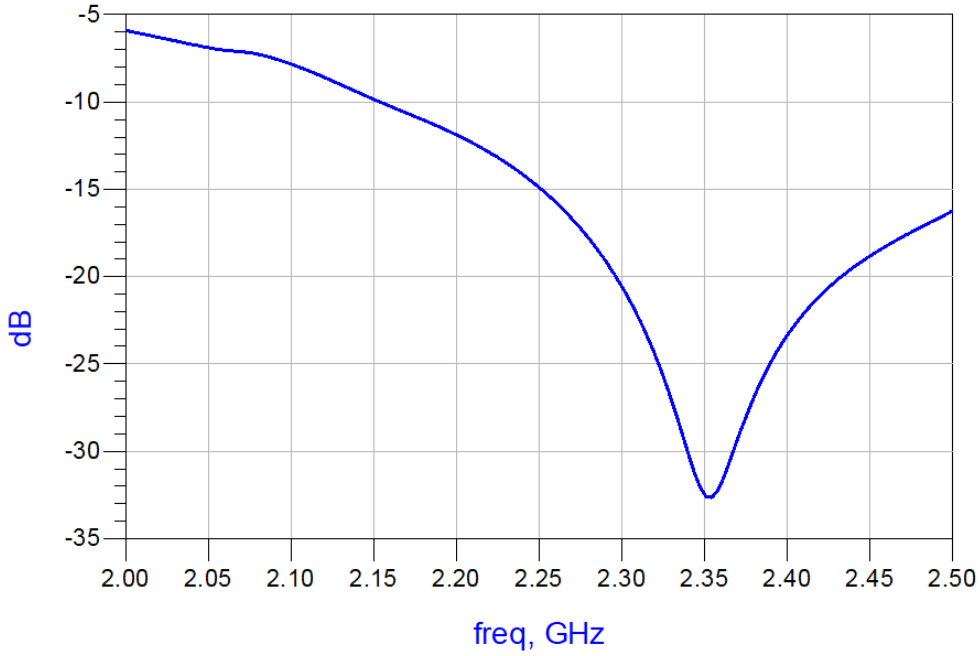


Figure 4.16: S_{22} parameter from simulation.

bandwidth window, the power is not always below $-10dB$, representing, still, a good bandwidth.

Considering the isolation of each port from each other, it is important to verify the behaviour of the designed system analyzing the S_{21} parameter. This parameter represents the power received at Port2 relative to the power input to Port1. In that way, how much lower this value is, the better, once lower values indicate lower interference between the two ports. Figure 4.17

It is possible to verify that for low frequencies, the interference between ports is lower. Considering the operating frequency, the power value it is $-20.5dB$. This means that if $1W$ it is delivered to Port1, then it will be delivered to Port2 about of $0.0089W$. This guarantees a good isolation between ports, avoiding interference's between RX and TX signals.

Also the phase of each layer was analyzed, in order to verify if the three coupled signals were coherent in phase, as also the three splitted signals. Figure 4.18 represents the phase for Port1 an Port2.

Inspecting the results, it is possible to verify that for each port, the three lines are matched in phase, which guarantees that will not exist a phase shift between the three signals. For Port2 there is a small deviation, but it is not enough significant to induce a big impact in the signal.

4.2.3 Power Divider/Combiner Construction

After the simulations, the designed was order to manufacture at the available shop in FEUP. Then, when the design was printed in the PCBs of FR4 substract, there was a work of cutting the layers with the hexagonal desired shape and holes for connections, as also a work of drilling and soldering the vias between the ground layer and the signal layers. For the vias, 2mm holes were made in the

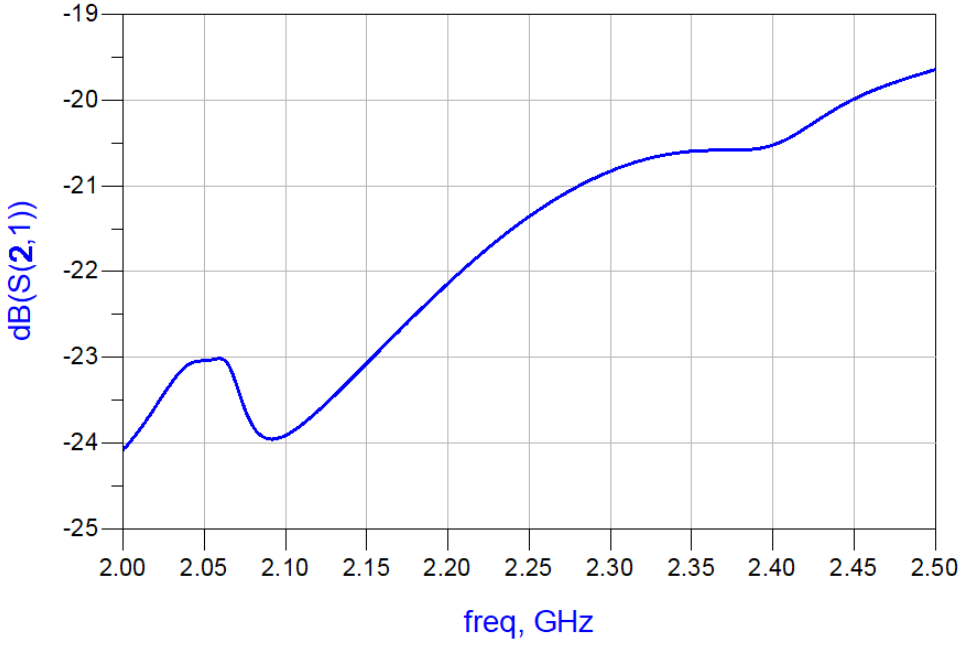


Figure 4.17: S_{21} parameter from simulation.

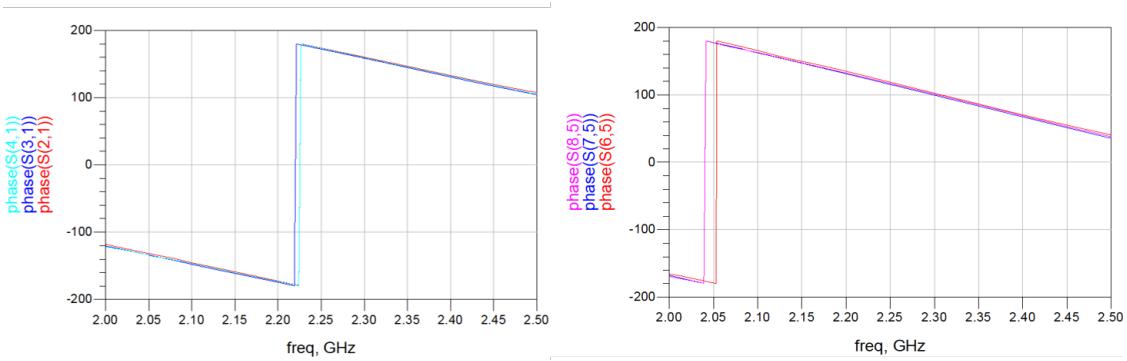


Figure 4.18: Phase plot for Port1 (left) and Port2 (right).

PCB, where were welded hollow conductor tubes also with 2mm of diameter and 1.6mm length for the vias that crosses only one layer, and 3.2mm for the ones that crosses over the two layers. Also it was drilled some holes in the top layer to avoid to the solder do not create a space between the two layers when attached. Other two holes were made in the bottom layer to allow to weld the SMA connectors and the coupling of the cables. The final PCB consists in the coupling of the two layers that are connected and properly attached to each other only by the vias. In figure 4.19 are shown the already coupled top (on the left), and bottom (on the right) layers of the PCB after the manufacturing process and mounting process.

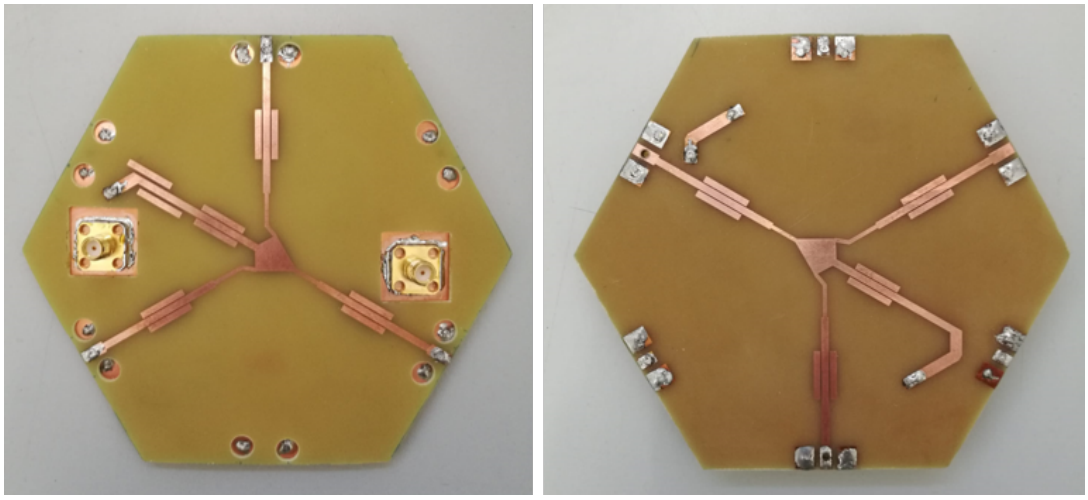


Figure 4.19: Power Divider/Combiner PCB.

Chapter 5

Feedback Interference Cancellation and ID System

In this chapter, the main focus is to study options for signal regeneration when a signal is under feedback interference. In order to mitigate this problem, it will be studied a few approaches that may have a good impact in this kind of problems. Also there is a focus to understand a way to detect which individual target in the field.

5.1 Feedback Interference Cancellation

When re-transmitting signals from a system that does not have a good isolation between the Rx and Tx signals, there is always a feedback interference that is created if the signals operate at the same frequency. This system oscillation may destroy the signal that is re-transmitted. In that way there should be a solution that can mitigate this kind of problems.

5.1.1 Regeneration Based on Signal Processing

In order to re-transmit a received signal with a higher gain to the SAR system, a signal processing system is a possible solution that can be implemented. Signal regeneration is the most clean way to improve a quality and power of a signal. In that way a block chain like the one represented in figure 5.1 could be a possible solution to regenerate the signal

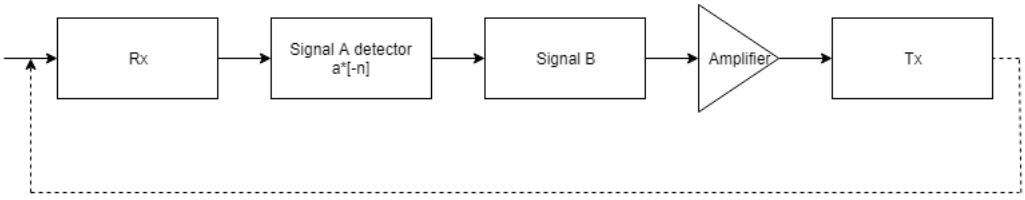


Figure 5.1: Feedback cancellation system

Figure 5.1 represent the received signal, the system to be implemented in the Active Target and the transmitted regenerates signal.

This approach may be addressed in the following way:

- The digital system allows to do a correlation with the signal A that is the signal transmitted by the RADAR and to be received in the Active Target.
- When received, the target affects the result with the signal B, which means that B is the impulse response of the correlation.
- Then, the signal is amplified by an amplifier and is transmitted back to the RADAR.

Both, signal A and B must be such, that auto correlation of $a[n]$ and $b[n]$ are impulse responses. In order to obtain a clean signal with no feedback interference, the cross correlation between $a * [-n]$ and $b[n]$ must be low. Find out and create a signal B that allows to generate a clean new signal,is the main concern to implement such a system. In this work there is no purpose to clean the signal making a study of the interference part and subtract it, as already exist in many systems.[16] The importance in this approach is to guarantee that this kind of system can still improve the gain of the signal comparing to simple repeater that just re-send the signal back

5.1.2 Regeneration Based on Frequency-Shifting and Filtering

Frequency shifting is one possibility that can really increase the gain of the re-transmitted signal, since the Rx signal suffers shift frequency and will re-send a signal with different frequency, which will not induce a feedback. However there is a concern in this approach, once the shift in the frequency will cause a phase lag. In SAR systems, a phase lag is a big concern, once this may create two images, but his is only an issue if it is considered that two or more active target are really close to each other, otherwise, it is possible to calculate the middle point between the two target images, and consequently identify the original target position. This can be a solution that can provide good results in terms of gain for the active target, and the problems may be mitigated, using some methods discussed further.

When a RADAR's signal is modulated with a reference sine signal it will cause a upper and a lower sideband. In this way, to clean the interference signal, and maintain the new shifted signal, a filter approach can be addressed to this problem. First of all it must be studied the impact of generating a frequency shift in the signal, in terms of generating a SAR image. The frequency shift, as already told will introduce an error in terms of target location in the image. To know how this impact will be relevant in the SAR post processing image, one should analyze it in terms of range and azimuth, that are the two dimensions of a SAR image. For this calculations will be assumed the following parameters will be assumed:

- Operating frequency: $f = 2.39GHz$
- Bandwidth: $B_w = 15MHz$

- Transmitting time: $T_{Tx} = 70\mu$
- Frequency Shift: $f_s = 25$MHz
- Clock Resolution : $C_r = 1$ppm (x2 due to emitting and receiving) =2ppm

$$\Delta f = \frac{2}{10^6} * 25 * 10^6 = 50Hz \tag{5.1}$$

$$Clock_{error} = \frac{50}{2.39 * 10^6} = 0.021ppm \tag{5.2}$$

$$Error_{range} = \frac{T_{Tx}}{B_w} \Delta f \frac{c}{2} = 0.035m \tag{5.3}$$

As it is possible to verify, applying a shift of 25MHz in the signal, will not cause any trouble to the correct place of the target in the image, since the error will be only 0.035m, which besides of being to small, is also considerable smaller than the SAR image resolution.

Analyzing now the error that could be associated to the azimuth resolution, the following considerations can be taken:

- Operating frequency: $f = 2.39GHz$
- Target Distance: $Dist = \sqrt{R^2 + x^2}$
- Range: $R = 737$km - for x=0 (x is the origin of axes corresponding to the sweep length that is performed from right-to-left or vice-versa), that is where *Dist* is bigger
- Scanned distance: $x = vt$
- Satellite Velocity: $v = 7500$m/s
- Transmitting time: $T_{Tx} = 70\mu$
- Frequency Shift: $f_s = 25$MHz
- Clock Resolution : $C_r = 1$ppm (x2 due to emitting and receiving) =2ppm
- Signal = $e^{-j2\pi(\frac{1}{\lambda_1}+\frac{1}{\lambda_2})Dist(t)}$

Doing the derivative of the signal that describes the one used in the system, it is possible to calculate the frequency of the

$$freq_A = (\frac{1}{\lambda_1} + \frac{1}{\lambda_2}) \frac{\partial Dist(t)}{\partial t} = (\frac{1}{\lambda_1} + \frac{1}{\lambda_2}) \frac{x}{\sqrt{R^2 + x^2}} v \tag{5.4}$$

Considering that the satellite is just above the target which means $x = 0$, and doing an approximation of the two wavelengths that are similar:

$$\frac{2xv}{\lambda R} = \Delta f \tag{5.5}$$

then

$$Error_{Azimuth} = x = \frac{\Delta f R \lambda}{2v} = 300m \tag{5.6}$$

In the case of azimuth, it is possible to verify that the induced error by the frequency shift it is significant for target location detection. Although the target can be detected, the same will have a position error of 300m, which can be critical depending on the Active Target use case. For example, if one is using the Active Targets in an environment where there is a considerable number of them in same area, it will not be possible to identify the precises location of the target, since they may be very close to each other. However, if the targets are far enough from each other, it is possible to measure the distance between the two symmetric images, and verify what is the middle point between them, and consequently one may determine the original position of the target. The solution for the very close targets will not be addressed in this work and will be considered as future work

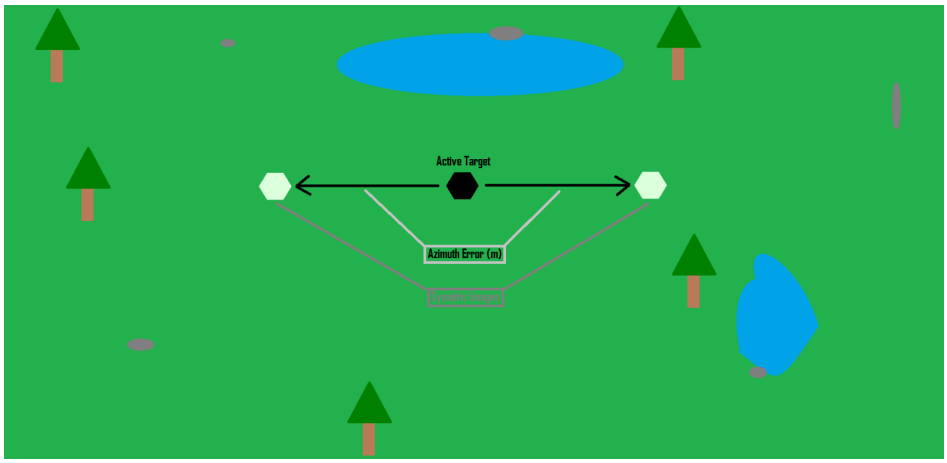


Figure 5.2: Errors form frequency shift: Symmetric Images of Target and Azimuth Error

To implement the frequency shift, a filter was designed in order to obtain the wanted results. First of all, it can be designed a band-pass filter that is used to filter the received signal, with the central frequency located at the received signal and with the respective bandwidth. This allows to clean the signal from the interference's added during the emission until the receiver.In order to obtain the frequency shift, and create two sidebands, one shifted for a low frequency, and other for a higher frequency. This step leads to a design of a second band-pass filter, that will filter the signal with the original frequency that may have been corrupted with the interference signal that leaded to the oscillation of the system. This dual-band filter will then allow to avoid the unwanted signal, and maintain the two sidebands shifted from the original signal. After the filtering process, the signal is re-sent back to the SAR system that will received a signal with a shift in its phase, originating two different images with the Active Target in two different locations. However, the gain that can be addressed to this method is quite significantly, once there is no interference between the received and the sent signal, which can provide an easy target detection relatively to the rest of the image.

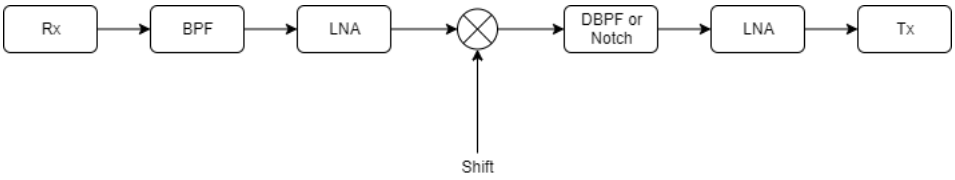


Figure 5.3: Frequency shift and filtering block chain

To ensure that a system like the one demonstrated in figure 5.3 is capable to introduced significant gain in order to be reliable for the wanted purpose, it is necessary to perform some calculations with the gains and losses introduced by each block, comparing the two different signals: signal 1 that is the original received wave with no shift, and signal 2 that is signal 1 after suffer a frequency shift of 25MHz up, and down, and after passing the a Notch filter that will only allows to pass the shifted signals and will attenuate the originate signal 1. Figure 5.4 represents the spectrum of the signal A and B.



Figure 5.4: Signal 1 at left and signal 2 at right

Comparing now the gains that each block will introduce to each signal it is possible to calculate the Active Target total gain, that will be important in the final link budget, and also verify if the system will oscillate or not. Figure 5.5 represents the possible paths of the signals, with the associated gain of each blocks. The represented gains are possible reference values of each block.

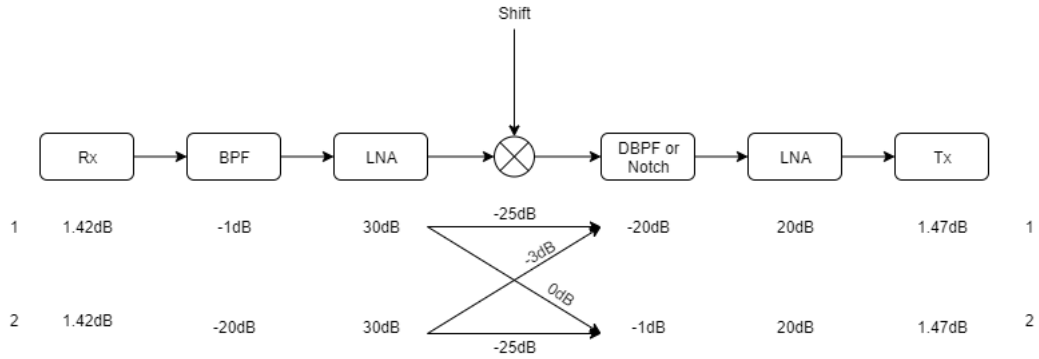


Figure 5.5: System block chain, and signals possible paths

For this study, it must be done four analyses corresponding to four paths signals:

- **1 to 1 and 2 to 2**: In this case is considered that the signal 1 is the emitted signal by the SAR system. When the signals arrives to target, the Rx antennas adds its own gain, that in this case is already the obtained gain by the RF designed system of this work as it will be

analyzed ahead in this document. After, the signal is filtered in the band-pass filter designed with the purposes to allow to pass only the emitted signal, avoiding to input interference's to the system, that may have been added to the original signal during its path until to the target. After, the LNA will introduce additional gain, before the signal passes trough the up/down converter without performing frequency shift, that has an RF to Output isolation gain of -25dB. As the signal was not shifted in the frequency, the Notch filter will induce a -20dB gain, once it is designed to attenuate at the frequency A. After a new LNA gain will be performed just before the additional gain of the Tx antenna. This chain allows to the system obtain $7dB$ gain. Also, to path B to B, the same value will be achieved as expected, once the only differences are in the band-pass and notch filter's that now exchanges its gains comparing to the previous path. 7dB gain a low value to the target, which makes unpractical for target identification purposes.

- **1 to 2**: In this case an analysis is made in which the original signal 1 is received and will be shifted originating the signal 2, where its power is divided in two side frequencies, remaining still some energy in the original frequency (A). Again, the signal arrives to target and will be added a gain associated to the Rx antennas. After, the filtering of the signal at frequency A, that aims to avoid some path interference's will be performed with its representative gain. The LNA will improve the gain of the signal, and the signal will pass trough the up/down converter to be shifted and originate the signal B1 and B2. In this case is considered a shift of 25MHz that is called the Intermediate Frequency, and allows to perform the up/down conversion with about 0dB gain, according to references values of components like the one considered. After the new signal with two side bands shifted 25MHz each, will pass trough the Notch filter that will allows to attenuate the amplitude at frequency A, allowing only to pass the two desired shifted signals(B1 and B2) and originating the new wanted signal 2. At last, signal 2 is amplified by the LNA and re-sent with an additional gain associated to the Tx antennas gain. This method allows to the Active Target perform a gain level of 51dB, that is a considerable good value for the purpose of this work.

- **2 to 1**: In this last analysis is considered that the signal 2 is received by the system at its entry, and added the additional gain of the Rx antennas. The band pass filter will input a -20dB gain, once will attenuate the two side frequencies (B1 and B2) it was designed to allow to filter the original signal A. After the LNA gain, the signal passes trough the up/down converter and will originate B1+25MHz which is not desirable and B1-25MHz=A, as also B2+25MHz=A and B2-25MHz which is not desirable. The unwanted frequencies has much gain as the resultant energy of signal A, and so a gain of -3dB will be added to the system. After the signal passes in the Notch filter and will attenuate again the originated signal that is similar to signal A. Finally there is again the input gain of the LNA and the Tx antennas. This allows to achieve a gain of 10dB, which is close to the gain obtained in 1 to 1 and 2 to 2 analysis.

After the previous analysis where 51dB was achieved for the Active Target, it necessary to do an analysis in terms of feedback for each possible signals path, to ensure that this system will not oscillate. To ensure that, it be considered that there is no oscillation when the obtained gain of the signal at its input stage is < -3dB, after the isolation of the ports. Figure 5.6 illustrates the feedback path and the isolation value between the port1 and port2 of the RF system, that corresponds to its calculated S_{21} parameter.

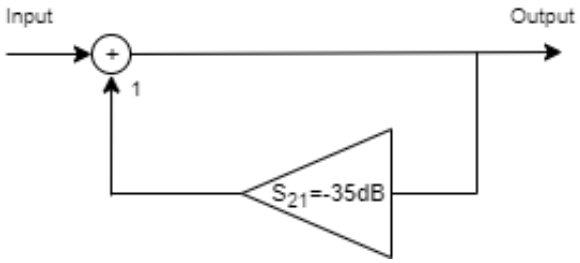


Figure 5.6: Feedback path and isolation between port2 and port1

- **[1 to 1 -> isolation] and [2 to 2 -> isolation]**:



Figure 5.7: [1 to 1 -> isolation] and [2 to 2 -> isolation] feedback paths

$$7 - 35 = -28dB < -3dB \tag{5.7}$$

It is possible to verify that for these both cases the feedback interference will not occur and the system meets the requirements.

- **[1 to 2 -> isolation -> 2 to 1 -> isolation]** :



Figure 5.8: [1 to 2 -> isolation -> 2 to 1 -> isolation] feedback path

$$51 - 35 + 10 - 35 = -9dB < -3dB \tag{5.8}$$

Again, is confirmed that this path also does not create feedback interference to the system, and allows to the Active Target to have 51dB gain without the system starts oscillating.

- **[2 to 1 -> isolation -> 1 to 2 ->isolation]**:



Figure 5.9: [2 to 1 -> isolation -> 1 to 2 -> isolation] feedback path

$$10 - 35 + 51 - 35 = -9dB < -3dB \tag{5.9}$$

As expected, this last path shows the same behaviour as the previous one, and meets the defined requirements, in which this kind of the system, with an Active Target of 51dB gain will not introduce feedback interference to the system.

The previous analyzed block design is composed by components that can be implemented and designed, and others can be bought from the of the shelf. The filters, as it should be passive, a microstrip approach is one method that can be implemented. In that way it is possible to design the two filters to achieve the wanted requirements. The LNAs can be bought of the shelf and the down-up converter too, with the only constrain to meet the defined requirements of the system.

5.1.2.1 Performed Tests with audio signals

Some tests in MATLAB were performed in order to verify if this solution could add value to the system in terms of its gain. However, this tests were performed for low frequencies that corresponds to the audible frequencies, once there was no possibility during this work to perform a test with radio-waves. It is known that the behaviour it is not exactly the same, but it can be made an explanation and a proof of the concept.

First of all it was designed as reference a FIR low pass filter (U_{p0}) with he following specifications: U_{p0}:

Low-pass FIR:

- Fs=44100
- Fpass:500Hz
- Fstop:1000Hz
- Apass=1dB
- Astop=40dB

Using this filter it was possible to generate the first band-pass(U_p1), that filters the original signal from path interference's:

$$U_{p1} = U_{p0} \frac{cos(2\pi(0 : length(U_{p0}) - 1)}{44100 * 7000} \tag{5.10}$$

This band-pass filter has the central frequency at 7kHz repeating at 37kHz, and the width of the passing band is 1kHz. It is possible to verify from figure 5.10 that the passing band has a difference of about 35dB comparing to the rejection band.

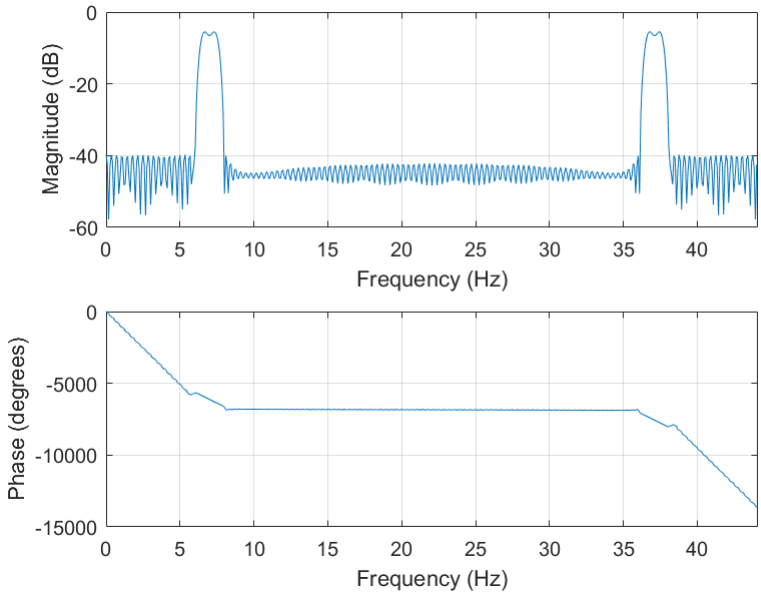


Figure 5.10: U_{p1} band-pass filter

After, it is generated the second band-pass filter also from the original U_{p0} filter:

$$U_{p2} = U_{p0} \frac{cos(2\pi(0 : length(U_{p0}) - 1)}{44100 * 5000} + U_{p0} \frac{cos(2\pi(0 : length(U_{p0}) - 1)}{44100 * 9000} \tag{5.11}$$

In this filter, the corrupted signal is filtered and the sidebands are allowed to pass trough the system, once this filter has a dual band-pass projected for the frequency shift.

As it is possible to verify from the figure 5.11 , the first passing band has its central frequency at 5kHz and the second at 9kHz, which means that here was a 2kHz shift to the right and left side of the spectrum on the original signal. The width of the passing band is now 500Hz, once now there is a dual band-pass filter. It is possible to verify that the magnitude difference from the rejected band and the passing band is also about 35dB. This gain is the one that can add value to the target regarding the signal regeneration process, and is very important to be high as possible.

This concept was tested in Simulink environment in which a system was designed that allowed to do it. Figure demonstrates the created environment.

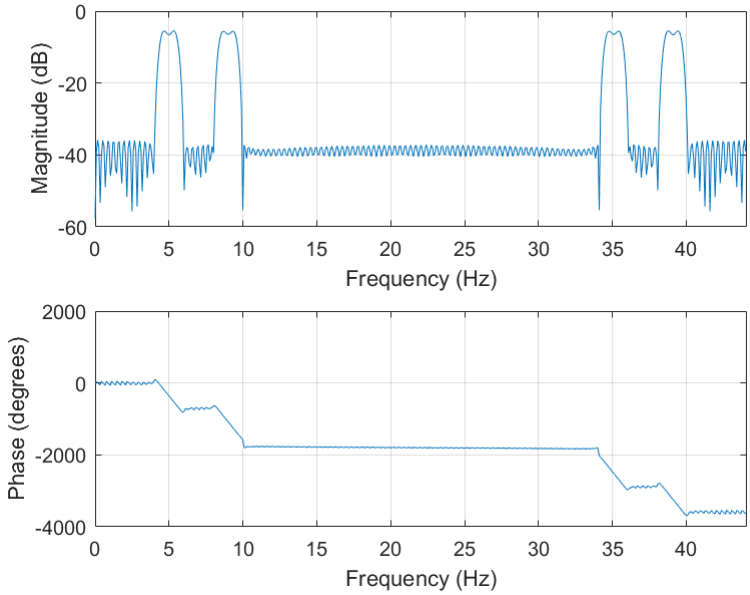


Figure 5.11: U_{p2} band-pass filter

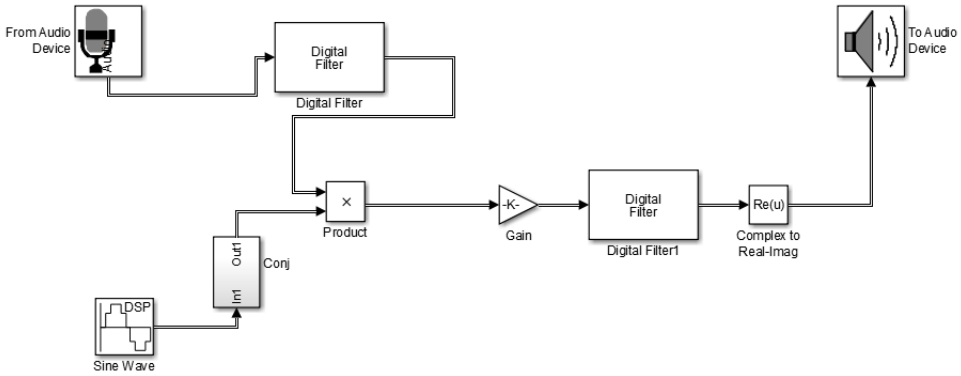


Figure 5.12: Simulink block chain for simulation.

This system was tested with sound signals, as also using a chirp. It was possible to verify that this system, comparing to one that does not have the filtering chain, has a much better performance. It was possible to verify that the filtering system only starts to oscillate with about 90 times bigger than a simple repeater system. This gain could still be bigger if the shift in frequency was even greater. However there are some restrictions to the bandwidth of the Active Target system, and a smaller shift in the frequency does not create a big error to the generated images.

5.2 ID system

When using an Active Target for targets detection in earth surface, besides locating it in the SAR image, it is also important to identify which information carries the spotted Active Target. So a

method for target *state* detection, which gives information of the *state* of the target carrier was performed.

One may consider a specific target, that is wanted to be tracked in the field, as also to know the condition of each one at the precise moment of the analysis: if the target is coupled to some device that detect the *state* of the target, the same can give to the Active Target an electric pulse correspondent to a specific *state* itself. This kind of monitoring is possible to be done.

Taking advantage of the frequency shift that is performed for signal regeneration, it is possible to address the shift in the frequency to a *state*. If each individual state has each own corresponding frequency shift, it is possible to know the state of the target by receiving the signal in the SAR system with its associated shift. E.g.: if the *state 1* is detected by the coupled device, the same will send to the Active Target an electrical signal that the Active Target will assume that is the one corresponding to do a 25MHz shift in the signal received by the satellite that will be re-sent back. At the satellite, the system will recognize that the frequency shift used was in the order of 25MHz, and already knows that this frequency shift means that the target was detected with the *state 1*. With this information it will be possible to to SAR system not only perform an image that demonstrates the position of the target, but also can provide information about the *state* of the detected target.

However, if it is addressed only one shift for each *state*, there will be a need to have a list with frequency shifts equal to the number of the *states*, which is unnecessary and may increase the resources of the Active Target which implies more complexity and power consumption. To avoid that, it can be performed combinations of frequencies: to each *state* 3 frequencies in a total universe of 5 frequency shifts values can be adressed. This means that with only 5 shift frequencies, for example, it is possible to achieve 10 different states:

$$N_{states} = C\binom{n}{x} \tag{5.12}$$

in which n is the number of available shift frequencies, and x is the wanted number of frequencies per *states*.

Chapter 6

System Integration Results

The system consists on an array of six antennas, three for each one of the two signals, as also its feeding network. Intrinsic to this system is the signal regeneration and target identification. In this section, it will be presented the characterization of the integrated target in terms of RF, where S-Parameters and radiation pattern were measured in the anechoic chamber at FEUP.

6.1 Target Integration and Tests

After all elements of the active target were ready, there was an assembling of the entire system. The first step was the assembling of the six antennas to the feeding network. First of all, there was a need to bend strips of a conductor that was welded to the antennas and the power divider, in order to achieve the correct angle and make sure that the antennas fit properly to the sides of the target structure. Each antenna was welded with three strips of the conductor (two for ground, and one for signal), and after that, there was also a last process of bending the strips for a last adjustment and correction of the angle between the antennas and the power divider for the attaching to the target structure. With this process, the array was finally complete and ready to be attached to the target structure. Figure 6.1 represents the entire array already complete.

With array already assembled, the same was attached to the target structure, and the active target was complete for a battery of tests consideringf RF performance. As already shown in chapter 3, figure 6.2 shows again the final result of the active target

When the active target was ready, several tests were performed in the anechoic chamber in order to verify the behaviour of the system, regarding with the previous simulations made. First of all, the S-Parameters of the target were analysed.

Figure 6.3 represents the S_{11} that is related to the Port1.

Considering these results, one can verify that just like the S_{11} of the patch antenna, the central frequency of the system associated to the Port1 is 2.38GHZ. However, it presents only of $-8.6dB$ in magnitude, which does not commits the $-10dB$ defined. This may happened due to the process of fabrication of the PCB and its construction, once everything was "hand-made" and some errors



Figure 6.1: Antenna Array and Power Divider.

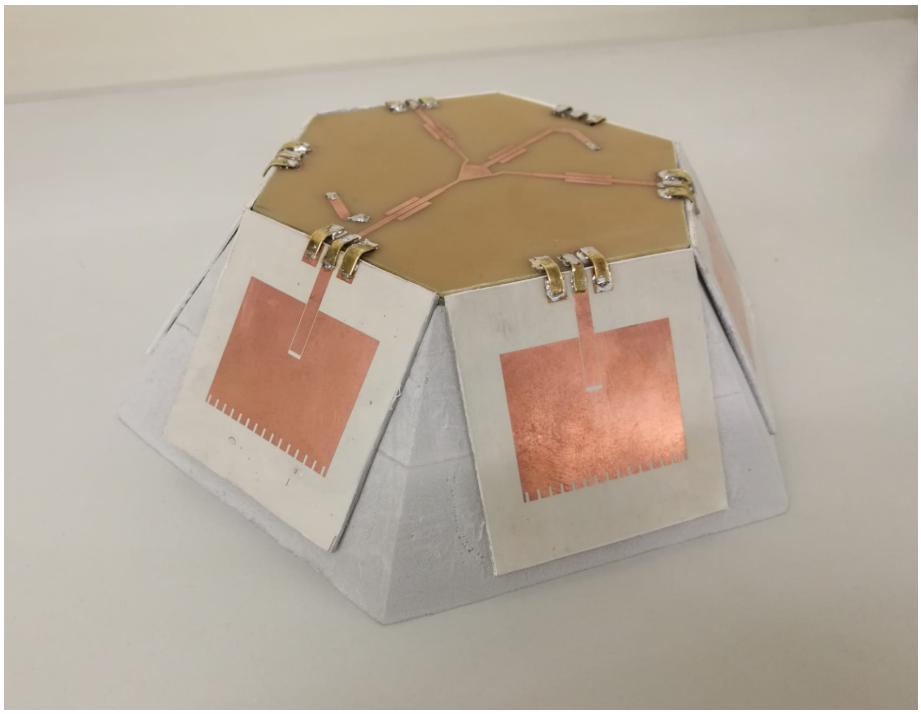


Figure 6.2: Active Target.

may be introduced to the PCB which leaded to some losses. Still, as it will be presented further in this document, this was not a big issue in a way that could impact significantly the system.

Taking in consideration the Port2 of the system, the S_{11} of the same that will be called as S_{22} is represented in figure 6.4

In this case, it is possible to see that the central frequency has a bigger shift comparing to the Port1, and it is now located at 2.41GHz. However, the magnitude at this frequency its $-14.9dB$

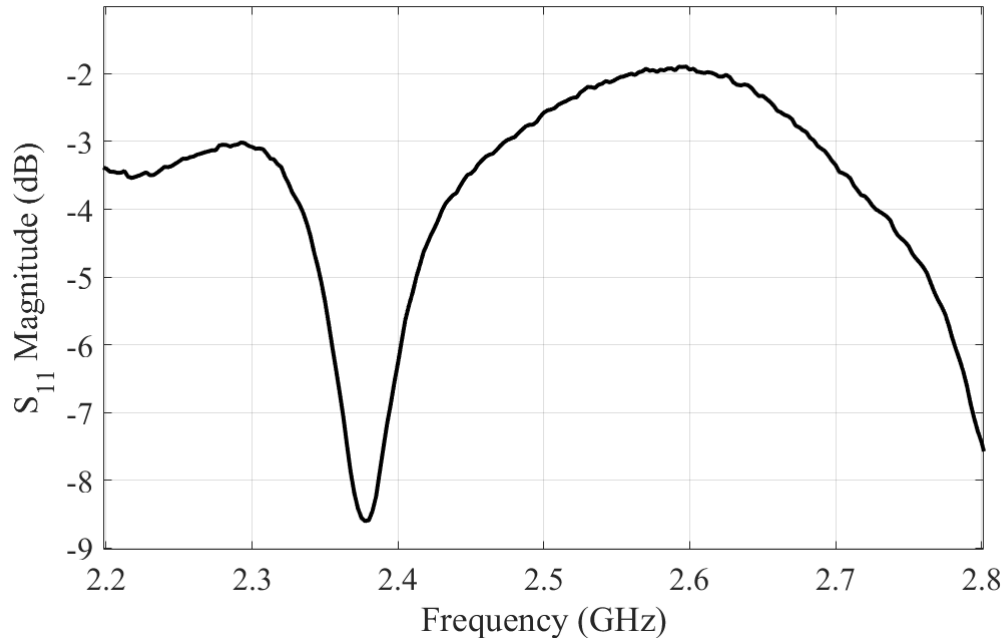


Figure 6.3: Measured S_{11} of Active Target

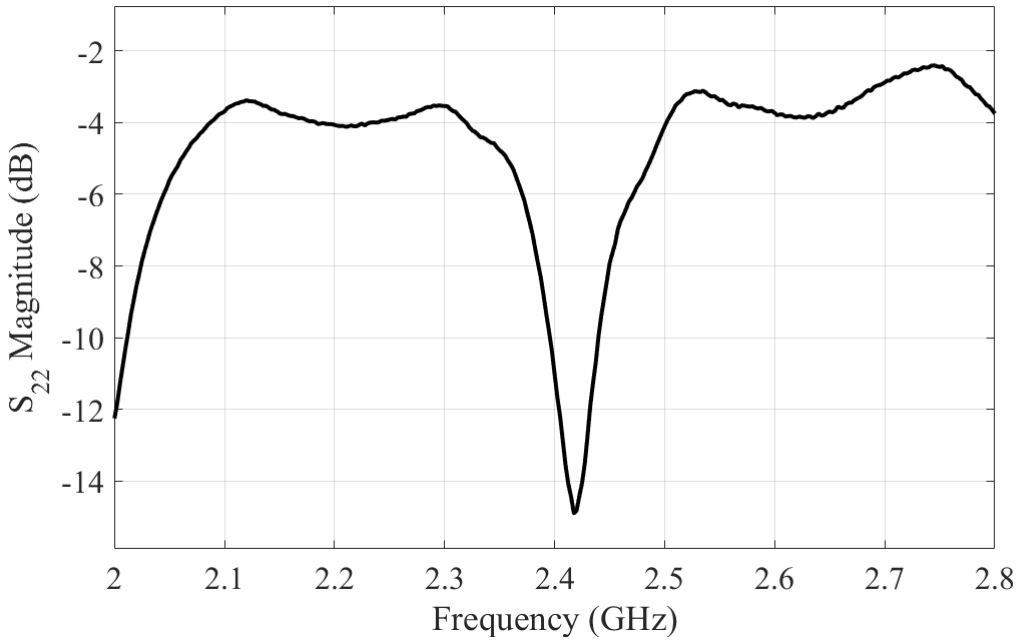


Figure 6.4: Measured S_{22} of Active Target

and the bandwidth is almost 30MHz. Again, some deviations of the central frequency may happened to successive accumulated small errors during the construction of the antennas and the PCB.

At last, the S_{21} of the system was analyzed in order to verify if the two ports are well isolated from each other. Figure 6.5 shows the obtained result.

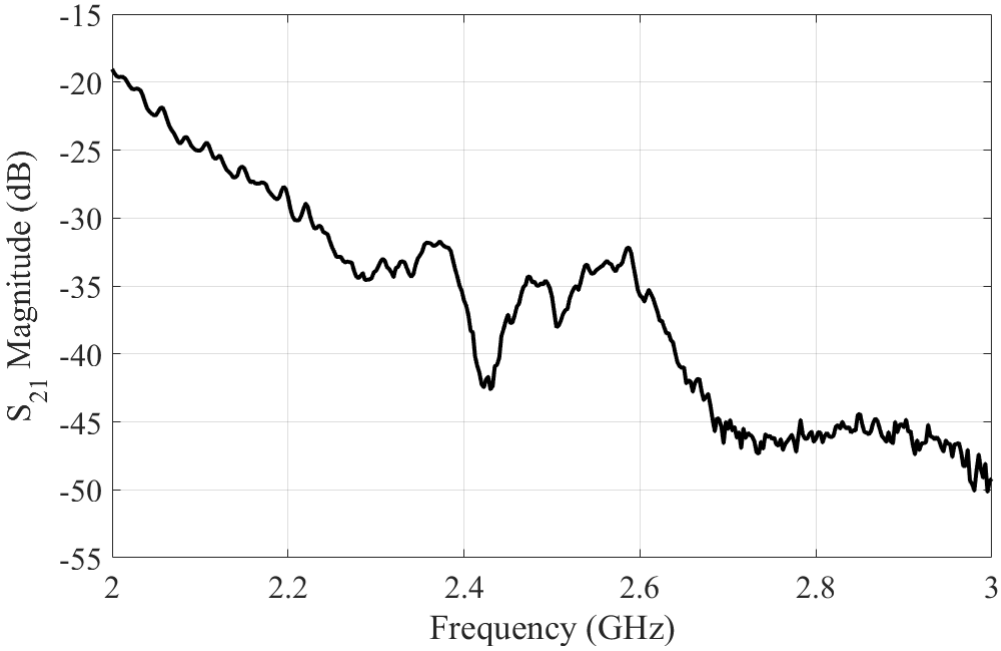


Figure 6.5: Measured S_{21} of Active Target

As it is possible to verify, for the range of the operating frequencies that has been analyzed during this work, the magnitude is between $[-35dB, -43dB]$ which although not to much constant frequencies, are good values of isolation from each port, even better than the expected EM simulations done with ADS. This means that applying 1W to one of the ports, the power delivered to the other port will be always at least less than 0.0003W.

The system was also characterized by the measurement of its gain and radiation pattern. To achieve that, was used a substitution method. First of all, it was used two similar Vivaldi antennas were mounted in front of each other in the anechoic chamber. Figure 6.6 illustrates the disposal of the antennas, and the distance from each other. With the set ready, it was measured the S_{21} and the distance between the two antennas. The distance allowed to calculated the free space path losses trough equation 6.1

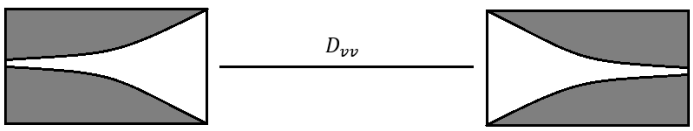


Figure 6.6: Schematic of the measurement of the two Vivaldi antennas

$$G_f = (\frac{\lambda}{4\pi R})^2 = (\frac{c}{4\pi R f})^2 \tag{6.1}$$

Considering that the distance D_{vv} is the distance between the two Vivaldi antennas, and it is 4.3m, the associated FSPL is $52.53dB$ considering $f = 2.35$GHz.

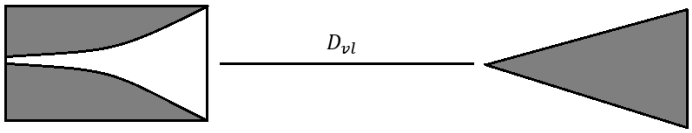


Figure 6.7: Schematic of the measurement of each Vivaldi antenna with the Log-Periodic Antenna

After this measurement, it was made a measurement of each Vivaldi antenna with a Log-Periodic antenna, as it demonstrates figure 6.7 , in order to obtain the gain of the each three antennas. For that it is possible to solve the following system:

$$\begin{cases} G_{v1} + FSPL_{D_{vv}} + G_{v2} = S_{21_{vv}} \\ G_{LP} + FSPL_{D_{vp}} + G_{v1} = S_{21_{v1p}} \\ G_{LP} + FSPL_{D_{vp}} + G_{v2} = S_{21_{v2p}} \end{cases}$$

Where G_{v1} and G_{v1} are the gain of Vivaldi 1 and 2 respectively, G_LP is the gain of the log periodic, $FSPL_{D_{vv}}$ is the FSPL associated to the distance between the two Vivaldis, and $FSPL_{D_{vp}}$ is the FSPL associated to the distance between each Vivaldi to the Log-periodic, once this antenna is bigger than the Vivaldis. Also, $S_{21_{v1p}}$, $S_{21_{vv}}$ and $S_{21_{v2p}}$ are the S_{21} parameters measured between the two Vivaldis, Vivaldi1 and Log-Periodic, and Vivaldi2 and Log-Periodic, respectively.

After calculated the gain of the Log-Periodic antenna that is $7.73dB$ and proceeding to the same schematic done previously, but now using the Active Target (figure 6.8) it is possible to achieve its absolute gain(6.2) trough equation where $FSPL_{D_{al}}$ are the FSPL associated to the distance between the Active Target and Log-Periodic.

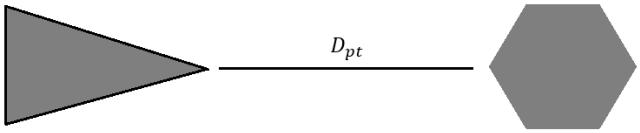


Figure 6.8: Schematic of the measurement between the Log-Periodic and the Active Target

$$G_{AT} = S_{21_{pt}} - FSPL_{D_{pt}} - G_{LP} \tag{6.2}$$

To create a 3D radiation pattern of the system, to know where the array radiates its energy, the Active Target was rotated against the Log-Periodic in the its own axes that crosses its center, from 0^o to 180^o with steps of 10^o. In each 10^o step position, the rotor where the antenna was placed, rotated also from -120^o to 120^o, as figure demonstrates.

The radiation pattern of the Active Target for Port1 can be observed in fig 6.10

With this 3D figure, one can verify that in the 360^o coverage of line of sight, there is a bigger radiation in three direction separated alternatively, that correspond to the three antennas connected to this port, as expected. Although it is possible see that one of them radiates more than the other

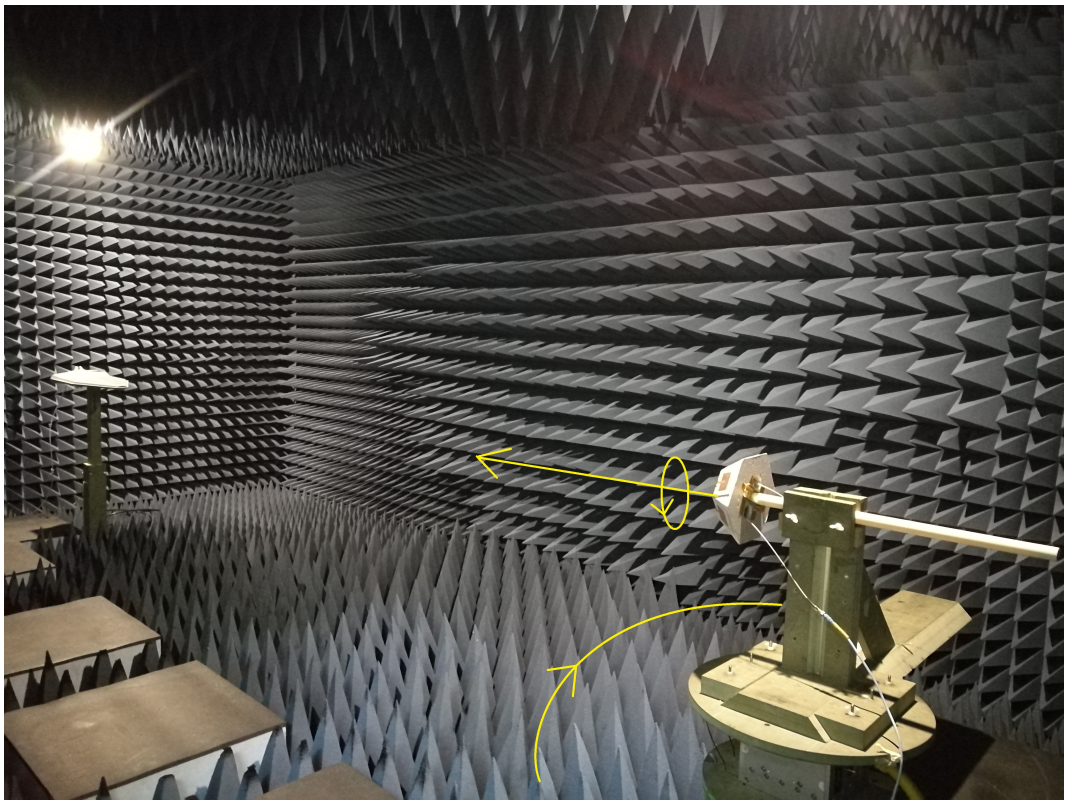


Figure 6.9: Graphical representation of rotation axes

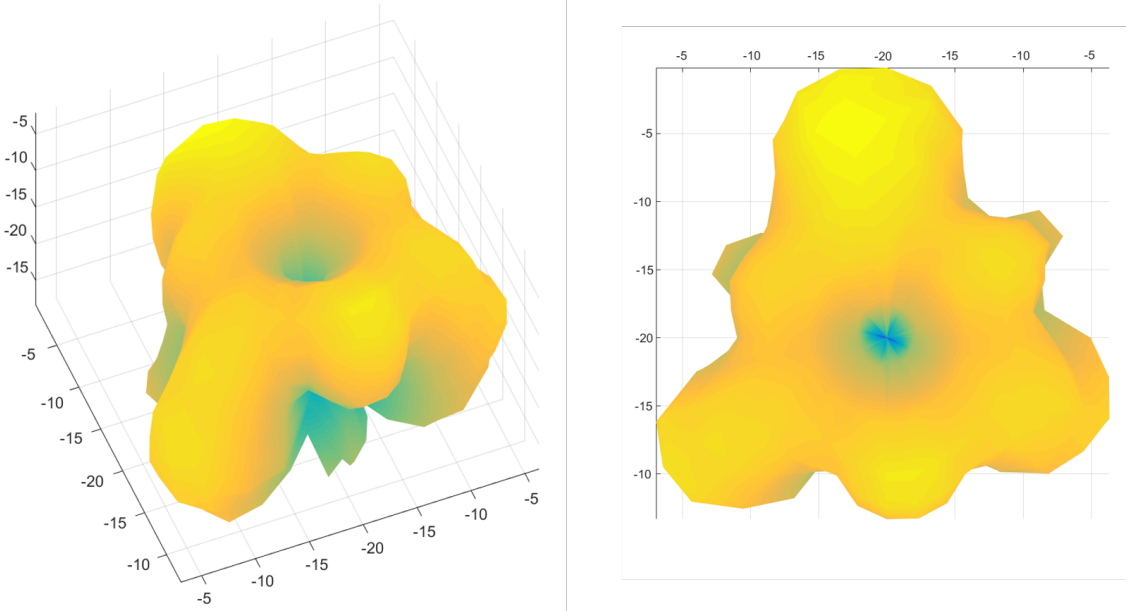


Figure 6.10: 3D Measured Radiation Pattern for Port1

two that are more similar to each other in terms of radiation pattern. Again this may occur due to some imperfections during the manufacturing process that introduced some errors.

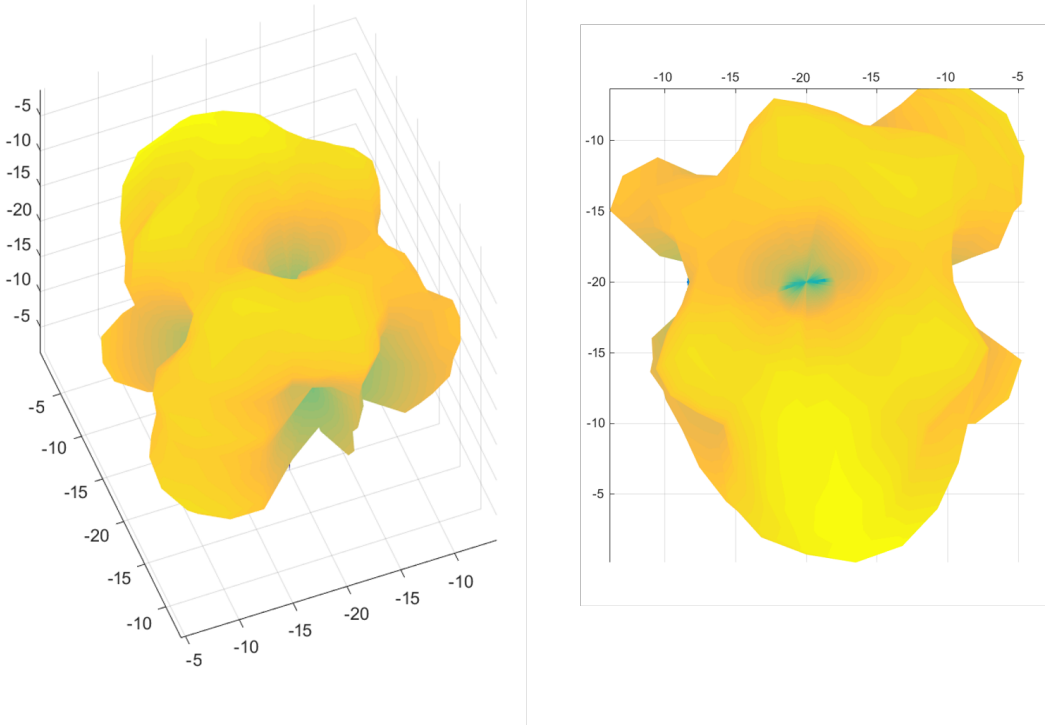


Figure 6.11: 3D Measured Radiation Pattern for Port2

At last, the 3D radiation pattern plot for Port2 is shown in figure 6.11

Again, the same phenomenon is verified in the radiation pattern where now the other three antennas associated to this port radiates much more than the other three. There are some side lobes which means that not all energy is being radiated efficiently.

Doing this analysis it was possible to obtain the values of gain of the Active Target array. Considering the Port1 , the maximum gain achieve is 1.68dBi in frequency of 2.38GHz. In Port2 the maximum gain is achieved at 2.41GHz with 1.90dBi of gain. This behaviour can be an interesting point when applying a method of frequency shifting between the received and transmitted signal, once the two ports have good gain values at different frequencies. However, the common frequency were the two ports has the better gain is at 2.39 GHz, in which Port1 has 1.47dBi and Port2 1.42dBi, and in this case the gain is also reasonable for an array of this kind, which means that using a method were there is signal regeneration without a shift of frequency, this tag can give a good response. The 3D charts presented corresponds both to this frequency.

6.1.1 System Performance

After the tests performed to the RF system and the analysis of signal regeneration for increased gain, it is possible now to do other analyzes based on the entire system performance, and the

capability of the Active Target to add value in terms of target recognition in SAR operation mode. In order to conclude if the Active Target complies with the environment that is exposed in a SAR system, a link budget analysis was performed.6.4.

Doing an analysis of the presented values on the link budget, the Tx Power is a reference used value for the chosen frequency band. The gain of Rx and Tx antenna corresponds to a parabolic dish with 1m of diameter for a $fc = 2.39$GHz, that is the frequency value with better results in the previous analysis of the Active Target.

Regarding the FSPL, the value obtained is the same for the ascending and descending path, at2.39GHz. With a flight altitude of 500km, and performing a stripmap SAR with 45^o angle from Nadir, the distance between the Active Target and the satellite is about 737km. Figure 6.12 is a schematic of the distances and angles of the environment, that must be considered during the following analysis.

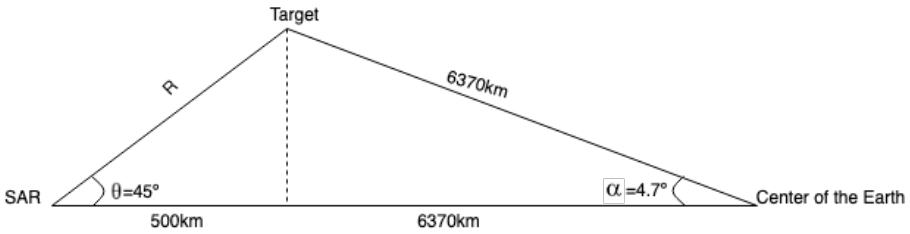


Figure 6.12: Positioning and geometry schematic of the entire system

$$FSPL = 20log_{10}(\frac{4\pi R}{\lambda})^2 = (\frac{4\pi * 737000}{0.1255})^2 = -158dB \tag{6.3}$$

The total gain of the Active Target was obtained by the sum of the gain of its Rx and Tx antennas for 2.39GHz, with the isolation factor between Port1 and Port2 and with the gain obtained in the signal processing by doing a shift in the frequency. This values were obtained previously and the achieved gain is given by:

$$G_{AT} = 51dB \tag{6.4}$$

The achieved gain addressed to the Active Target is quite significant for the system, and may add a big value to the purpose that this is work stands for. A gain of approximately 51dB already calculated in the previously chapter, is a good result, where the RF system and signal processing system achieved both good quality indicators.

The noise figure associated to several system losses in the receiving may also be considered in this calculation.

Johnson–Nyquist noise must be considered and is associated to the system due to the thermal agitation of the electrons. Considering a temperature T of 300K, a bandwidth B of 15MHz and the Boltzmann constant $k_B = 1.38 * 10^-20$ it is possible to calculated it by the given equation:

$$Noise = K_B TB = 10log_{10}(1.38 * 10^{-20} * 300x * 15 * 10^6) = -102dB \tag{6.5}$$

At this stage it was already possible to calculate the Signal to Noise Ratio by adding the Total Power achieved at the receiving of the system, with the Noise:

$$SNR = -149 + (-102) = -47dB \tag{6.6}$$

There are additional gains in a SAR system, after receiving the scattered signal. As already discussed in this work, the processing process of a SAR image is directly related with the data associated to the azimuth and range compression. This processing has an associated compression gai given by:

$$G_{R_C} = BT_{Tx} = 10log_{10}15 * 10^6 * 70^{-6} = 30dB \tag{6.7}$$

where B is the bandwidth of the signal and $T_{Tx}$is the transmission time of the impulse.

Also, the azimuth compression only depends on the number of pulses that are transmitted, and those ones depends of the following equation:

$$N_{Pulses} = \frac{PRF^2 \lambda R}{2v^2} \tag{6.8}$$

in which PRF is the pulse repetition frequency used in the system that in this case is considered as 1kHz, λ is the wavelength, R is the distance of the SAR system to the target that is 737km, and v is the velocity of the satellite with the SAR system that for LEO orbit was considered as 7.5km/s. This parameters allow to achieve a number of pulses of 800, which leads to a gain of:

$$G_{A_C} = 10log_{N_{Pulses}} = 29dB \tag{6.9}$$

Finally, it is possible to calculate the gain margin that is achieved with the Active Target when used in a SAR approach, which would be the sum of the SNR with the additional processing gain. Table 6.4 shows the Link Budget of the system.

Table 6.1: System Link Budget using 45^o Nadir angle

Designation	Value	Unit
Tx Power	60	dBm
Tx Antenna Gain	30	dB
Forward FSPL (@737km)	-158	dB
Active Target	51	dB
Backward FSPL	-158	dB
Rx Antenna Gain	30	dB
Noise Figure	-5	dB
Total	-150	dBm
Noise	-102	dBm
SNR	-48	dB
Range Compression Gain	30	dB
Azimuth Compression Gain	29	dB
Margin	11	dB

The achieved gain margin with this system is 11dB, which is a good value when thinking the purpose of this work. However, and considering that the frequency shift system is implemented, it must be considered the losses introduced by the up-down converter, that is about 3dB, decreasing the gain margin to 8dB margin.

However a link margin of 8dB was achieved: it is possible to increase this margin by reducing the Nadir angle. Reducing the Nadir angle will have an impact in the distance between the SAR system and the target, once the distance will be smaller and the FSPL will decrease, but also because will increase the azimuth compression gain because the PRF will also increase and consequently the number of pulses too. However, it is not possible to decrease the Nadir angle too much in a way that could achieve 0^o, because the range resolution will decrease and the SAR image will be deteriorated. With the parameters used in this link budget it is possible to calculate the range resolution achieved by:

$$R_{range} = \frac{c}{2BW}\frac{1}{sin(\theta+\alpha)} = 13m \tag{6.10}$$

This obtained range resolution for the SAR image is good enough for the proposes that this system is designed for, and can provide sufficient good resolution for SAR images.

All the previous analysis were made considering a Nadir angle of 45^o and this will be considered as the maximum angle to not compromise the link margin. It is possible to do now an analyse for two different angles: 30^o that will be considered as nominal, and 15^o as limit to not reduce too much the resolution range.

- Nadir angle = 30^o

Considering the same altitude of 500km but now with a Nadir angle of 30^o, the distance between the target and the satellite is 585km, achieving a FSLP of:

$$FSPL = 20log_{10}(\frac{4\pi R}{\lambda})^2 = (\frac{4\pi * 585000}{0.1255})^2 = -156dB \tag{6.11}$$

To calculate the new achieved azimuth compression gain, one must calculate the new PRF first, that depends on the target area length obtained with the previous Nadir angle and the angle originated from the earth curvature that was achieved performing calculations based on the previous figure 6.12 , as also on the impulse time that is again $70\mu s$, both paths.

$$PRF = \frac{1}{\frac{Target_l}{\frac{c}{2}} + 2T_{Tx}} = 2KHz \tag{6.12}$$

Knowing the new PRF it is now possible to calculate the new number of pulses:

$$N_{Pulses} = \frac{PRF^2\lambda R}{2v^2} = 2496 \tag{6.13}$$

The azimuth compression gain achieved is now:

$$G_{A_C} = 10log_{N_{Pulses}} = 34dB \tag{6.14}$$

Performing again the link budget with the new achieved values:

Table 6.2: System Link Budget using 30º Nadir angle

Designation	Value	Unit
Tx Power	60	dBm
Tx Antenna Gain	30	dB
Forward FSPL (@585km)	-156	dB
Active Target	51	dB
Backward FSPL	-156	dB
Rx Antenna Gain	30	dB
Noise Figure	-5	dB
Total	-146	dBm
Noise	-102	dBm
SNR	-44	dB
Range Compression Gain	30	dB
Azimuth Compression Gain	34	dB
Margin	20	dB

With 30º Nadir angle it is possible to increase the link margin to 20dB which is a big improvement comparing to the previous achieve link margin. Subtracting again the losses induced by the up/down converter, its achieved a link margin gain of 17dB.

However it must be considered the range resolution that is achieved with this parameters, to verify it does not degrades too much, in a way that could compromise the SAR image resolution:

$$R_{range} = \frac{c}{2BW}\frac{1}{sin(\theta+\alpha)} = 18.5m \tag{6.15}$$

As expected, the range resolution achieved is worst than the previous case, but can still perform a SAR image that does not compromises its quality.

- Nadir angle = 15º

Doing the same procedure it is possible to achieve the following:

$$FSPL = 20log_{10}(\frac{4\pi R}{\lambda})^2 = (\frac{4\pi * 519000}{0.1255})^2 = -155dB \tag{6.16}$$

$$PRF = \frac{1}{\frac{Target_l}{\frac{c}{2}} + 2T_{Tx}} = 3.5KHz \tag{6.17}$$

$$N_{Pulses} = \frac{PRF^2\lambda R}{2v^2} = 6780 \tag{6.18}$$

$$G_{A_C} = 10log_{N_{Pulses}} = 38dB \tag{6.19}$$

With these new values it is possible to perform the following link budget:

Table 6.3: System Link Budget using 15º Nadir angle

Designation	Value	Unit
Tx Power	60	dBm
Tx Antenna Gain	30	dB
Forward FSPL (@519km)	-155	dB
Active Target	51	dB
Backward FSPL	-155	dB
Rx Antenna Gain	30	dB
Noise Figure	-5	dB
Total	-144	dBm
Noise	-102	dBm
SNR	-42	dB
Range Compression Gain	30	dB
Azimuth Compression Gain	38	dB
Margin	26	dB

Again, as expected, was achieved an improvement on the link margin, by 6dB with respect to the previous, given by 23dB after the induced losses by the up/sown converter. At last, the new range resolution is:

$$R_{range} = \frac{c}{2BW}\frac{1}{sin(\theta+\alpha)} = 35.8m \tag{6.20}$$

However the obtained link margin has a very good value, it can be verified that in this case the range resolution achieved a value that may deteriorate the SAR image and would not be possible to have big details in the image. In order to have a balance between the link margin and the range resolution, the 30º Nadir angle may be the one that can provide better results in this type of system. Still, and depending on the purposes of the usage, it is possible to choose an angle that provides higher target detection on the environment where the resolution of the image it is not crucial, or an angle that can provide lower target detection, but still possible to detect, but have a high resolution image.

Considering the frequency shift approach for signal amplification, the performance of the RF system and the parameters of SAR operation defined in the previous link budgets, it is possible to verify that the Active Target can achieve a good gain of margin, which make possible to be identified in the environment when processing a SAR image, making it useful for the purposes of specific target identification. Te link margin of 17dB allows to say that the target reflects 17 more times energy comparing to the environment.

6.1.2 Power Consumption

In terms of power consumption, there is a very simple layout of the system regarding the devices that consumes energy. The antennas, the power divider and the filters are all passive, so, the only components that may consume some power are the LNAs and the Up/Down converter. Taking as

reference, some LNAs and up/down converters that meets the wanted requirements it was possible to achieve the following values:

Table 6.4: System Power Consumption

Component	Voltage (V)	Max Current (mA)	Power (W)
Up/Down Converter	3.3	440	1.45
LNA_1	4.5	80	0.36
LNA_2	4.5	80	0.36
Total	-	600	2.17

It is possible to verify the power consumption it is only 2.17W, and the reference devices are not the optimized ones, being possible to find others with lower power consumption. However, the calculations in this work will be made with this values that are the worst case scenario.

Assuming that a LEO satellite is equipped with a SAR system has is orbit at 500km of altitude, and travels with 7.5km/s speed, its orbit period will be about 1:30h. However the orbit it is not the same during the time, and has a upward and downward way, which makes the satellite to pass in the line of sight of the Active Target 1 time every 12h. Considering also that the duration of a SAR performance is about of 20 seconds, it will be assumed that the target will be turned on 1min per each satellite passage in order to be sure that is detected. With this values, it is possible to say that per each day the, each target will be turned on only for 2 minute per day. However to increase the number of times that the targets can be detected, it could be used a constellation of satellites that would allow to monitor the target much more times per day.

The design of a system that could provide to the target the knowledge to turn on every each pass of the satellite it is out of the scope of this analyzes, but many approaches could be done, such as installing a low power consumption micro-controller with a GPS that could give information about the next satellite pass, and wake up the target, or even allow to the Active Target to receive e short impulse form the satellite that could wake up the tag.

If to this Active Target uses a power supply based on a regular 9V battery, attached to a voltage divider to be possible to achieve the voltage inputs of the components, with a capacity of 600mA/h associated to a 600mA discharge that only occurs 1 minute per day, it is possible to say that the battery will last about one month. Still, this duration time could be even improved if a small solar panel that can provides energy to the system is attached to the system. With this results it is possible to implement a low power consumption Active Target that can still commit the requirements for what was designed, being reliable for tracking and monitoring targets.

Chapter 7

Final Remarks

7.1 Adversities during the work development

During the development of this thesis, some setbacks occurred. The first one was during the simulations performed for the design and tuning of the antennas. With a limited gain and bandwidth that this kind of antennas could perform, a lot of simulations that take a lot of time were needed to perform with iterative steps. However the main difficulties encountered during the simulations performed for the RF component occurred in the power divider simulations. This was a very intensive process that took a couple of months to achieve the wanted results. Each simulation took almost an hour and the process of tuning it was all performed with iterative process of small changes in the design, once the Power Divider design was not at all a typically one due to the structure requirements for the Active Target. Also, the constructions of the antennas and the power divider was challenging, since the available equipment to cut it and get assembled was not the most adequate one. All of the work has hand made, which became difficult to replicate the system as it was simulated, leading to some variations in the real measured parameters of the system. At last, there was an additional challenge to find a way to fix the active target in the rotor in the the anechoic chamber in a way that could be simple and easy to do all the rotations for the measuring of the radiation pattern, which led to an extra work of constructing an attachment between the Active Target and the rotor.

7.2 Conclusions

Design and construct an Active Target for SAR applications, capable to be easily detected in the environment, trough RF and signal processing solutions, was a challenge. It is not properly a trivial problem find way to build an array capable to add a reasonable gain to system, and not even try to solve the feedback problem in a way that the same could be minimize to increase significantly the gain of the system. After the performed work for this thesis, here presented, it is possible to achieve a developed concept of an Active Target for SAR applications with a good performance, even with some restrictions. This constructed Active Target is able to be integrated

with a similar feedback cancellation solution also presented in this work, in order to be attached to a wanted target to be identified from a passing satellite or a airbone. The performed tests proved that this developed system can be a potential method to perform this kind of target identification with success.

Along this dissertation, was presented a detailed study of the type of structure to assemble the system, the antennas array for receiving and transmitting signals, possible solutions for feedback interference cancellation, and also an identification solution for the target, that could be used for the purpose of the presented objective. The way that the structure should be design and constructed is explained and justified in order to achieve mounting and performance requirements. Also, and depending on that, the design of an antenna unit that could meet the desired performance requirements is designed, simulated and also constructed for post analysis as an array. Once there was an array in the system, there was also a need to do a design and simulation of a power divider that could combine and split the Tx and Rx signals from each antenna in the array. After designed, a PCB was constructed in order to be assembled to the antennas and feed the array. With this, the RF system of the active target was ready to be tested, and achieve real results.

After the RF system, a study of possibilities to cancel the feedback issue in the system was also performed. Some proposals of doing it were presented in this thesis, in which filtering process was the solution that had a bigger focus, and that is proposed to be assembled to the Active Target, once it proved that could create a good response in terms of adding gain to the complete system. At last also a target ID solution was studied and showed that it may be a good and simple solution to implement, by taking advantage of frequency shift. It is important to say that the design of the feedback cancellation system was performed after the construction and designed of the RF system, and it was possible to conclude that the needs of bandwidth of the feedback cancellation system were slightly bigger than the bandwidth that the implemented RF system could provide. Nevertheless, the purposes and veracity of this work are still completely valid, existing just a need to re dimension the design of the antennas and the power divider/combiner to achieve the wanted bandwidth-

Final RF tests were made, based on the design and construction of the RF system, the S-Parameters were taken form the VNA available in the university. Also, it was possible to perform 3D radiation pattern of the array in the anechoic chamber, to verify the real behaviour of the system, in which the results were reasonable good.

Even though it was not possible, for reasons of time, to perform a complete test of the complete assembled system in real conditions, it was possible to achieve good results in the performance of the RF sub-system and those ones are granted. The feedback and ID solution were the ones that were not possible to add to the RF sub-system, but a study and analysis on that was performed, and the results achieved indicated that the solutions is promising and has a high probability to meet the requirements of the complete system. In that way, it is possible to conclude that the presented work can be a potential solution for target identification in a SAR platform, and the main objectives of this thesis were achieved.

7.3 Future Work

Nowadays SAR systems are getting more importance and applications for remote sensing systems enabling to obtain high resolution RADAR images, regardless of weather condition, and from that, targets identification may be an interesting approach to monitor wanted targets on earth surface. This work aimed to be a step towards to perform an Active Target that could be used for that purposes.

To this system be totally reliable and used without constrains and with good data quality, it is important to perform some more tests focused on the feedback cancellation models purposed, to verify it in real conditions. Also, could be performed simulations based on more efficient antennas and power divider, but more important, do a rigorous and accurate construction of it, in a way to be possible to induce less losses and even higher gains, but also completely meet the requirements of the feedback cancellation system. At last could be done a study and analysis on a simple system that after the frequency shift for feedback cancellation was performed , allows to detect the precise position of the tag when numerous tags are close to each others.

Appendix A

Active Target technical draw

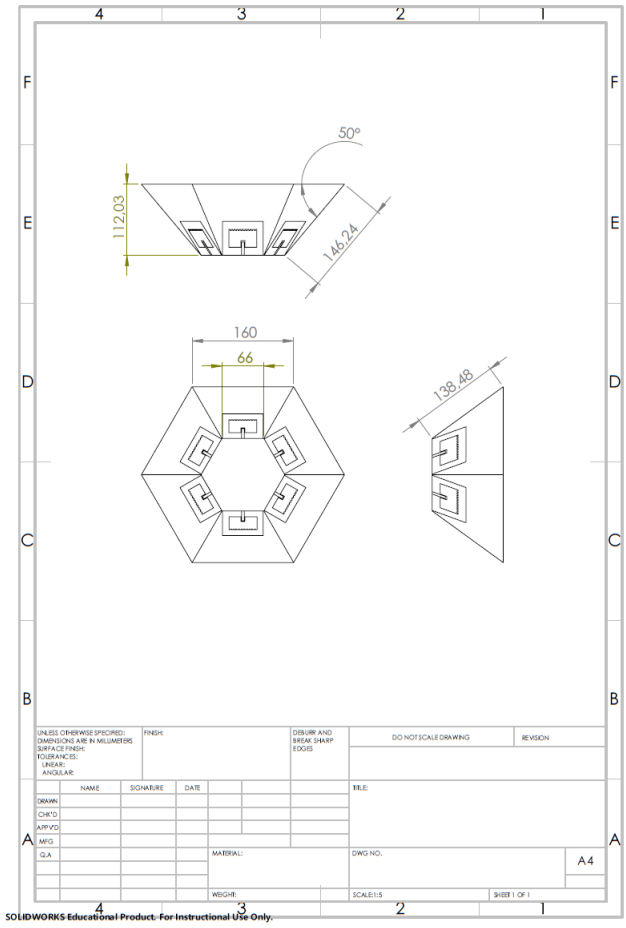


Figure A.1: Active target technical draw.

References

[1] A. Moreira, P. Prats-Iraola, M. Younis, G. Krieger, I. Hajnsek, and K. P. Papathanassiou. A tutorial on synthetic aperture radar. *IEEE Geoscience and Remote Sensing Magazine*, 1(1):6–43, March 2013. doi:10.1109/MGRS.2013.2248301.

[2] D. R. Brunfeldt and F. T. Ulaby. Active reflector for radar calibration. *IEEE Transactions on Geoscience and Remote Sensing*, GE-22(2):165–169, March 1984. doi:10.1109/TGRS.1984.350610.

[3] B. J. Doering, P. Looser, M. Jirousek, M. Schwerdt, and M. Peichl. Highly accurate calibration target for multiple mode sar systems. In *8th European Conference on Synthetic Aperture Radar*, pages 1–4, June 2010.

[4] M. Jirousek, B. J. Döring, P. Looser, and M. Schwerdt. First measurement results of a new highly-accurate active sar calibration target. In *2012 IEEE International Geoscience and Remote Sensing Symposium*, pages 1618–1620, July 2012. doi:10.1109/IGARSS.2012.6351219.

[5] M. Lee, B. Keum, H. S. Lee, and J. Kim. A radio repeater interference cancellation model for mobile communication systems. In *2008 The Fourth International Conference on Wireless and Mobile Communications*, pages 376–381, July 2008. doi:10.1109/ICWMC.2008.16.

[6] Constantine A. Balanis. *Antenna Theory: Analysis and Design*, volume 1. John Wiley & Sons, 2005.

[7] David M. Pozar. *Microwave Engineering*. John Wiley & Sons, 4th edition, 2009.

[8] D. D. Clark. Overview of the argos system. In *Proceedings OCEANS*, volume 3, pages 934–939, Sep. 1989. doi:10.1109/OCEANS.1989.586711.

[9] A. Moreira and G. Krieger. Spaceborne synthetic aperture radar (sar) systems: state of the art and future developments. In *33rd European Microwave Conference Proceedings (IEEE Cat. No.03EX723C)*, volume 1, pages 101–104 Vol.1, Oct 2003. doi:10.1109/EUMC.2003.1262228.

[10] B. J. Doring, P. R. Looser, M. Jirousek, and M. Schwerdt. Reference target correction based on point-target sar simulation. *IEEE Transactions on Geoscience and Remote Sensing*, 50(3):951–959, March 2012. doi:10.1109/TGRS.2011.2162590.

[11] D. H. Schaubert, D. M. Pozar, and A. Adrian. Effect of microstrip antenna substrate thickness and permittivity: comparison of theories with experiment. *IEEE Transactions on Antennas and Propagation*, 37(6):677–682, June 1989. doi:10.1109/8.29353.

[12] G. Chen, J. Sun, S. Huang, and YD Chen. The novel 3-way power dividers/combiners structure and design. In *2006 IEEE Annual Wireless and Microwave Technology Conference*, pages 1–4, Dec 2006. doi:10.1109/WAMICON.2006.351957.

[13] S.S.Chorage, Shilpa V.Joshi, Harshada S.Ahiwale, and Archana M. Gaikwad. Design and performance analysis of 1:6 power divider for l band frequency. *International Journal of Wireless Networks and Communications*, 8(1):15–21, 2016.

[14] C. Ortega. Argos second and third generations: enhancements finely tuned to oceanographic applications. In *IEEE Oceanic Engineering Society. OCEANS'98. Conference Proceedings (Cat. No.98CH36259)*, volume 2, pages 845–848 vol.2, Sep. 1998. doi:10.1109/OCEANS.1998.724357.

[15] A. Metin, D. Delikanli, İ. Kaya, S. Keskiner, T. Imeci, and T. Durak. Serration effect on gain for microstrip e-shape patch antenna. In *2016 IEEE/ACES International Conference on Wireless Information Technology and Systems (ICWITS) and Applied Computational Electromagnetics (ACES)*, pages 1–2, March 2016. doi:10.1109/ROPACES.2016.7465474.

[16] E. Ahmed and A. M. Eltawil. All-digital self-interference cancellation technique for full-duplex systems. *IEEE Transactions on Wireless Communications*, 14(7):3519–3532, July 2015. doi:10.1109/TWC.2015.2407876.